



## Chapter 6

# Summary & Conclusions

## Summary & Conclusions

Recent development in nanotechnology requires  $\text{PbWO}_4$  material having different morphologies and dimensions suitable for nano dimensional devices. So it is important to study effect of different reaction parameters (Precursor, pH, Concentration, Time and Temperature) on morphology of the final product.

We have prepared undoped as well as Cerium doped  $\text{PbWO}_4$  phosphor with various morphologies using facile Low Temperature Hydrothermal method. Self-designed Teflon Lined Stainless Steel Autoclave having 90 ml capacity was used to prepare all samples. We have divided our experiment into *two parts* to do systematic analysis of structural and optical properties of undoped and Cerium doped Lead Tungstate ( $\text{PbWO}_4$ ) phosphor. In the first part of our experiment undoped as well as Cerium doped  $\text{PbWO}_4$  phosphor were synthesized with different Lead sources (Lead Acetate, Lead Nitrate and Lead Chloride),  $\text{Na}_2\text{WO}_4$  as a metallic cation and distilled water as solvent. In the second part of our experiment  $\text{PbCl}_2$  was kept constant as a Lead source and phosphor were synthesized by varying reaction temperatures and pH of solution. Crystal structure, phase and morphology were characterized by X-ray Diffraction (XRD) Analysis Technique, Scanning Electron Microscopy (SEM), Transmission Electron Microscopy (TEM) and Photoluminescence. Lattice parameters, unit cell volume and average crystallite size were performed with PowderX program.

### Effect of Lead Sources

X-ray spectra of  $\text{PbWO}_4$  and  $\text{PbWO}_4\text{:Ce}$  synthesized  $100^\circ\text{C}$  temperature with different Lead sources are polycrystalline in nature and contain mixture of two phases

i.e. stolzite and raspite phase of  $\text{PbWO}_4$ . All X-ray diffraction peaks were indexed to a tetragonal stolzite phase with space group  $I4_1/a$  and monoclinic raspite phase with space group  $P2_1/a$ . The highest relative intensity is obtained for (112) crystallographic plane of tetragonal crystal structure. At  $100^\circ\text{C}$  temperature raspite phase is produced predominantly and with increase in temperature it transforms irreversibly into stolzite phase. Using  $\text{Pb}(\text{CH}_3\text{COO})_2$  as a lead source, large amount of raspite phase was produced compared to  $\text{Pb}(\text{NO}_3)_2$  and  $\text{PbCl}_2$ .  $\text{PbWO}_4$  prepared with Lead Chloride showed highest crystallinity and contained least amount of raspite phase inclusions. Hence *Lead Chloride proved to be better Lead source to produce high crystalline  $\text{PbWO}_4$  crystals over Lead nitrate and Lead acetate.* Range of unit cell volume for stolzite phase is  $359.47\text{-}383.83 \text{ (\AA)}^3$  and that is for raspite phase is  $359.09\text{-}375.32 \text{ (\AA)}^3$ . It is observed in our analysis that volume of unit cell of tetragonal and monoclinic structures are very close to each other; the difference is less than 0.53%. The average crystallite sizes were estimated by the Scherrer's equation using the Full Width at Half Maximum (FWHM) from the most intense peak (1 1 2).

The effect of different Lead sources on the morphology of  $\text{PbWO}_4$  was investigated from TEM and SEM characterization. Many interesting morphologies were produced in our experiments without the use of expensive template or surface directing capping agents. When  $\text{Pb}(\text{CH}_3\text{COO})_2$  was used as the lead source, product with mixture of two phases (stolzite and raspite) were produced.  $\text{PbWO}_4$  prepared with Lead Acetate possesses mixed morphologies of single branched dendrite around  $5\mu\text{m}$  long and tetrahedron microparticles are about 500 nm in size. When  $\text{Pb}(\text{NO}_3)_2$  was used as the Lead source, six branched dendrite ( $2.10 \mu\text{m} \times 1.18 \mu\text{m}$ ) and rhombic shaped particle and flat nanobelt ( $5\mu\text{m} \times 1\mu\text{m}$ ) were produced. When  $\text{PbCl}_2$  was used as the Lead source, octahedron shaped microparticles of having size around 100 nm

were produced and flat nanobelts having width 100-150nm and about few  $\mu\text{m}$  in length were obtained due. We assumed that dendrite, tetrahedron, rhombic and octahedron shaped microparticles are possesses stolzite phase of  $\text{PbWO}_4$ . Similarly nanobelts are possesses raspite phase of  $\text{PbWO}_4$ . As soon as both reactants mixed in supersaturated aqueous solution nanoparticles of  $\text{PbWO}_4$  were formed. Nanoparticles were assembled to form nanorod and nanoflake like structure when such mixture was treated in the autoclave for shorter duration of time. If we increase the reaction time for (12 h), rhombic shaped microparticles were produced which turns into single or multiple branched dendrite or flat microbelts. We can also conclude that at lower temperature raspite phase is produced and with increases in temperature raspite phase turns into stolzite phase. In general, *two phases of  $\text{PbWO}_4$  (stolzite and raspite) are produced irrespective of Lead sources at low temperature ( $100^\circ\text{C}$ ) and both phases produced have different morphologies in micrometer range.* The formation various morphologies of  $\text{PbWO}_4$  is attributed to favourable thermo-dynamic conditions. The formation and evolution processes can be divided into three steps: initial nucleation process in supersaturated solution, self-assembly process (oriented aggregation), and subsequent crystal growth process (Ostwald ripening).

Photoluminescence spectra of  $\text{PbWO}_4$  were investigated at room temperature using a 305-nm excitation wavelength. PL emission spectra of  $\text{PbWO}_4$  consists two components, a fast blue component around 450 nm which is an intrinsic feature of stolzite phase and a slow green one around 480-520 nm which is an intrinsic feature of raspite phase. A broad blue luminescence peak around 450 nm originates from tetragonal  $\text{WO}_4^{2-}$  groups. The dendrite with six branched structure, rhombic shaped nanoparticles and nanobelt have highest surface to volume ratio compared to single branched dendrite and tetrahedron microparticles, hence they

contain higher concentration of surface related defects (particularly oxygen vacancies) which enhance PL emission of  $\text{PbWO}_4$  prepared with Lead Nitrate compared to  $\text{PbWO}_4$  prepared with Lead Acetate. Photoluminescence spectra of  $\text{PbWO}_4$  prepared with Lead Chloride shows higher intensity compared to Lead Acetate and Lead Nitrate. The shape of PL spectra of  $\text{PbWO}_4$  synthesised using  $\text{PbCl}_2$  has “*spread-eagle-shape*” with a central peak surrounded by two broad shoulder peaks. Emission spectrum reveals that it is composed of several sub-bands which are almost distributed throughout entire 350-550 nm region. We proposed that the Gaussian peak I (367 nm), the Gaussian peak II (392 nm) and the Gaussian peak III (452 nm) may correspond to the radiative transitions from  $^3\text{A}_1 \rightarrow ^1\text{A}_1$ ,  $^3\text{A}_2 \cong ^3\text{E} \rightarrow ^1\text{A}_1$  and  $^3\text{A}_2 \rightarrow ^1\text{A}_1$ , respectively. Hence *blue emission occurs from the lower lying triplet state split by Jahn-Teller interaction. The peak position of all the three blue Gaussian components in PL spectra recorded at room temperature is shifted towards the short wavelength side compared to those reported at lower temperatures.*

### Effect of Cerium doping on $\text{PbWO}_4$

XRD reflection spectra confirm that Cerium doping in  $\text{PbWO}_4$  does not distort its characteristic shape. *Cerium doping in  $\text{PbWO}_4$  prepared with different Lead sources does not change the crystal structure or induce a new phase.* Cerium doping reduces lattice parameters of all  $\text{PbWO}_4$  samples prepared with different Lead sources.  $\text{Ce}^{3+}$  substitute well  $\text{Pb}^{2+}$  in  $\text{PbWO}_4$  lattice and induce  $\text{Pb}^{2+}$  vacancy in order to keep the charge neutral. The  $\text{Ce}^{3+}$  ions are likely to enter  $\text{PbWO}_4$  crystal lattice to substitute  $\text{Pb}^{2+}$  sites considering that the ion radius of  $\text{Ce}^{3+}$  (0.103 nm) is similar to that of  $\text{Pb}^{2+}$  (0.120 nm). Cerium suppresses the intensity of XRD peaks representing raspite phase. Hence we conclude that *Cerium act as catalyst and helps raspite phase to convert into*

*stolzite phase when Lead Chloride was used as Lead source.* Effect of  $\text{Ce}^{3+}$  doping on crystal structure of  $\text{PbWO}_4$  at different temperatures is not reported till date and first time we have done this type of study. It is also inferred from the XRD spectra that with Cerium doping, intensity of peaks representing raspite phase decreases and intensity of peaks representing stolzite phase increases. This behaviour is observed in all the samples for all the temperatures. Thus we can conclude that along with temperature, cerium also plays an important role to decrease the amount of raspite phase and increase the amount of stolzite phase with increase in temperature. The cell parameters, unit cell volume and average crystallite size of Cerium doped  $\text{PbWO}_4$  crystals at 100°C, 150°C and 200°C temperatures were investigated. It is found that lattice parameters and unit cell volume decreased with doping of Cerium at all temperatures. *Cerium increases the average crystallite size for more than 50% at all temperatures.*

Cerium doping in  $\text{PbWO}_4$  synthesized with Lead Acetate changes morphology to nanobelts ( $5\mu\text{m} \times 1\mu\text{m}$ ) having bamboo-leaf-like morphology. Growth mechanism of  $\text{PbWO}_4$  microbelt explained. Cerium will not play any direct role in the production of belt like structure. These nanobelts are produced at comparatively low (100°C) temperatures for short (12h) reaction time at 7pH. It shows that  $\text{PbWO}_4$  nanobelts can be produced at lower temperature without using any surfactant/capping agent or composite salt by hydrothermal method. Preparation of Cerium doped  $\text{PbWO}_4$  using Lead Nitrate as a Lead source is not reported yet by any other method except us with hydrothermal method. Cerium doping in  $\text{PbWO}_4$  synthesized with Lead Nitrate as well as Lead Chloride produces tetrahedron shaped  $\text{PbWO}_4$  nanoparticles having 100nm in size. Cerium doping in  $\text{PbWO}_4$ , tetrahedron shaped microparticles with stolzite phase is dominantly produced over raspite phase.

Thus Cerium plays an important role in controlling the morphology of  $\text{PbWO}_4$  prepared with Lead Nitrate and Lead Chloride. So we proposed that *Cerium plays the role of surfactant or capping agent by regulating crystal growth direction. This is a very interesting phenomenon and it should be investigated for other types of rare earth elements also.*

The intensity of PL is suppressed to a great extent by doping with cerium. The cerium doped  $\text{PbWO}_4$  shows weaker luminescence intensity than that of undoped  $\text{PbWO}_4$ . Green emission of  $\text{PbWO}_4\text{:Ce}$  prepared with Lead Acetate is more compared to  $\text{PbWO}_4\text{:Ce}$  prepared with Lead Nitrate which is assumed to related with respite inclusions. Photoluminescence emission spectra shows structured character for both undoped and cerium doped samples. Such type of structural shape invokes presence of four Gaussian components: three peaks fall in blue region and one in green region. The presence of four Gaussian components indicates the excited states of emission center are relaxed and degenerated under the influence by perturbation. According to Kobayashi et al. Cerium doping in  $\text{PbWO}_4$  results low energy shift of absorption spectra due to  $4f \rightarrow 5d$  transitions and hence emission spectra should also shift to lower energy side due to Stokes shift. Similar type of red shift is observed in position of Gaussian peak IV in our case. Furthermore, decrease of light yield (LY) for  $\text{PWO:Ce}$  sample by a factor 2–3 was observed with respect to undoped PWO. The absence of intrinsic  $\text{Ce}^{3+}$  emission at the room temperature and observed lower Light Yield can be explained by a non-radiative  $5d \rightarrow 4f$  transition to the ground state of excited  $\text{Ce}^{3+}$  ions, i.e.  $\text{Ce}^{3+}$  ions can serve as efficient non-radiative traps in the PWO matrix. Such a conclusion support the observed faster PL decay of  $\text{PWO:Ce}$  at room temperature (RT) with respect to the undoped sample, which can be explained by

selective suppression of the delayed recombination process due to non-radiative recombination of free electrons and holes at the  $\text{Ce}^{3+}$  sites.

### Effect of pH of reaction solution on $\text{PbWO}_4$

To study the effect of pH of solvent on structural and optical properties of  $\text{PbWO}_4$ , three samples were selected which are prepared at 3pH, 7pH and 11pH.  $\text{PbWO}_4$  synthesized at different pH of reaction solution are single phase. X-ray diffraction analysis of these samples shows that all three samples are highly crystallized and completely indexed to a pure tetragonal stolzite phase of  $\text{PbWO}_4$  with space group  $I4_1/a$ . This result shows that the *different pH promotes the formation of crystalline  $\text{PbWO}_4$  powders at low synthesis temperature and reduced processing time than the other conventional methods.*

In order to analyze morphology of these samples with TEM, two samples (samples prepared at 7pH and 11pH) were chosen based on their excellent photoluminescence spectra.  $\text{PbWO}_4$  prepared at 7pH and 11pH show better crystallization than the one made at 3pH. Our result shows that  *$\text{PbWO}_4$  nanomaterials with good crystallinity can be formed even at 11pH and optimal pH range for  $\text{PbWO}_4$  is 3-11 pH.* TEM images shows that Quasi-spherical hallow nanoparticles (HNPs) with an average diameter of about 20-40 nm and hollow nanotubes (HNTs) having outer diameter approximately 12.37 nm and length around 80-170 nm were produced at 7 pH. Upon rising pH to 11, solid nanorods were produced with increased length from 80-170 nm to 2 $\mu\text{m}$  with 40 nm outer diameter. Formation of hollow nanoparticles (HNPs) and hollow nanotubes (HNTs) explained on the basis of Kirkendall counter diffusion effect. *Formation of  $\text{PbWO}_4$  Hollow Nano Tubes (HNTs) have not been reported yet, hence we are first to synthesis it. XRD and TEM analysis*



*shows that in the 7-11pH range highly crystallized 1-Dimensional PbWO<sub>4</sub> nanorods with pure stolzite phase obtained.* From the present work, it is found that the pH value of reaction system has great influence on the morphologies of the obtained samples, when the other conditions were the same. Regarding to the formation mechanism of the PbWO<sub>4</sub> nanorods through hydrothermal approach, it is clear that the growth process is not surfactant-assisted or template-directed, because no surfactants or templates are introduced into the reaction system. It can be noted from our result that *with increase in pH, size of PbWO<sub>4</sub> nanoparticles and length of the PbWO<sub>4</sub> increases and morphology changes from HNTs to nanorods.*

In order to study the effect of pH of the reaction solution on luminescence property, PL spectra of PbWO<sub>4</sub> synthesized at different pH was recorded at two excitation wavelengths 300 nm and 254 nm. PbWO<sub>4</sub> shows “spread-eagle-shaped” broad luminescent emissions in blue and green range. PbWO<sub>4</sub> (Nanoparticles and HNTs) obtained at 7pH, display a strong emission peak cantered at about 485 nm at room temperature. However, the absolute luminescence intensity increased with increasing pH, over the range of 3-7 pH, implying that the hollow nanoparticles (HNPs) and hollow nanotubes (HNTs) had much improved luminescence intensity. Very weak PL intensity of the sample obtained for 3pH due to poor crystallinity. Obtained PL spectra was fitted with four individual Gaussian peaks having peaks position for peak I (365 nm), peak II (395 nm), peak III (459 nm) and peak IV (500nm). Gaussian peak I, the Gaussian peak II and the Gaussian peak III may correspond to the radiative transitions from  $^3A_1 \rightarrow ^1A_1$ ,  $^3A_2 \cong ^3E \rightarrow ^1A_1$  and  $^3A_2 \rightarrow ^1A_1$ , respectively. The Gaussian peak IV ascribed to oxygen deficient irregular WO<sub>3</sub> neutral molecule. The PL intensity of blue and green emission peak is highest for sample prepared at 7pH (HNTs), it is intermediate for sample prepared at 11pH

(Nanorods) and lowest for sample prepared at 3pH which indicates that  $PbWO_4$  HNTs have more regular lattice structure, uniform morphology and highest defect centres relative to oxygen (due to faster 1-D crystal growth) compared to Nanorods. Sample prepared at 3pH has lowest regular lattice structure and lowest defect centres relative to oxygen.

### Effect of synthesis Temperature on $PbWO_4$

In order to study the effect of reaction temperature samples synthesized at four different temperatures: 100°C, 125°C, 150°C and 200°C were selected.  $PbWO_4$  prepared at 100°C temperature contains highest amount of raspite phase compared to those prepared at 150°C and 200°C temperatures. With increase in temperature from 100°C to 200°C percentage of raspite phase of  $PbWO_4$  decreases. Among all samples, pure stolzite phase produced only at 125°C with highest crystallinity. However, on comparing the XRD peaks of the products, we found that the relative intensity of the peaks varied significantly, indicate that at different temperature  $PbWO_4$  with different crystallinity forms. Thus different reaction temperature in our experiment would bring about significant changes in the crystallization of stolzite phase of  $PbWO_4$ . Lattice parameter (a, b) is highest for sample prepared at 100 °C which decreases with increase in temperature up to 150 °C and again increase for sample prepared at 200°C. While lattice parameter (c) remains constant for sample prepared at 100 °C to 125 °C and increase and become maximum for 150 °C then again decrease for sample prepared at 200°C. Unit cell volume is highest for sample prepared at 100 °C which decreases with increase in temperature up to 125 °C and again increase for sample prepared at 150°C. Unit cell volume then remains constant up to 200 °C. While

average crystallite size is highest for sample prepared 125 °C and decrease for 150 °C then again increase for sample prepared at 200°C. From our results we can conclude that *unit cell volume is inversely proportional to average crystallite size*.

To investigate the effect of temperature on morphology of undoped  $\text{PbWO}_4$ , TEM images of samples prepared at two different reaction temperatures i.e 100°C and 125°C were selected. TEM photographs of product obtained at 100°C temperature shows mixture of microparticles of octahedral shape having size around 100 nm as well as aggregation of nanoflakes like structure having width 100-150nm and about few  $\mu\text{m}$  in length. When the temperature rose to 125 °C, Quasi-spherical hollow nanoparticles (HNPs) having average diameter of about 20-40 nm and Hollow Nano Tubes (HNTs) having outer diameter 12.37 nm and around 80-170 nm in length with uniform and smooth surface were obtained. These HNPs and HNTs are highly crystalline compared to product obtained at 100 °C. Octahedraon microparticles and nanoflakes obtained at 100°C contains mix phases of stolzite and raspite structures, while Hollow nanoparticles and HNTs produced at 125 °C are of pure stolzite phase with high crystallinity. *Comparison of these products shows that at low temperature (around 100 °C),  $\text{PbWO}_4$  microstructures containing mix morphologies influenced by raspite as well as stolzite phase will obtained. As we go from low temperature to high temperature raspite phase is diminished and nanostructures with lower dimensions having pure stolzite phase is obtained.*

Room temperature photoluminescence spectra of  $\text{PbWO}_4$  nanophosphor prepared at different temperatures (100°C, 125°C and 200°C) were recorded with 254 nm and 300 nm excitation wavelengths. It is well known that PL intensity has direct relation with crystallinity. The better crystallinity, the higher PL emission peak is. Hence among all three samples (HNTs) of  $\text{PbWO}_4$  prepared at 125 °C shows strong

green luminescence due to its highest crystallinity while (microparticle + microplates) of  $\text{PbWO}_4$  prepared at 100 °C shows weak luminescence due to poor crystallinity. Higher crystallinity of Quasi-spherical nanoparticles and Hollow Nano Tubes are main reason to produce high PL intensity compared to low crystalline microparticles and flake like inclusions. It implied that  *$\text{PbWO}_4$  nanostructure have a better luminescence intensity then microstructure at room temperature. Higher intensity of blue emission at low temperature* shows that samples prepared at low temperature has higher concentration of  $\text{WO}_4^{2-}$ . At higher reaction temperature lattice regularity breaks and also decreases the concentration of blue emission center. Enhancement of Green emission of the sample prepared at 125°C is due to presence of larger amount of surface defect is also discussed.

### Up Conversion emission

Up-conversion emission was observed in undoped  $\text{PbWO}_4$  synthesized with different pH and temperatures excited with 625 nm wavelength, respectively. Intensity of up-conversion luminescence is highest for  $\text{PbWO}_4$  sample prepared at 7pH or 125°C, intermediate for 11pH and lowest for 3pH. Up-conversion luminescence intensity is also least for sample prepared at 100°C and 200°C.

Large single crystals of  $\text{PbWO}_4$  are produced either via Czochralski or Bridgman method which require highly expensive and specially designed equipments. These methods produce  $\text{PbO}$  and  $\text{WO}_3$  harmful gases during crystal growth due to higher synthesis temperature (i.e. 1125°C). Products obtained by these methods are in bulk size which cannot be used for devices based on nano dimensions. These limitations lower the applicability of these methods for large scale production of  $\text{PbWO}_4$  crystals. Shortcomings of high temperature synthesis techniques such as:

inhomogeneity, production of harmful gases, impurity contamination and powders with different sizes and non-uniform distribution of  $\text{PbWO}_4$  can be resolved by Low temperature Hydrothermal method. Thus *Hydrothermal process is proved to be effective, facile and green route for the synthesis of  $\text{PbWO}_4$  nanostructures having low-cost, high efficiency and good potential for high-quantity production.* Unlike many advanced methods that can prepare a large variety of forms, the respective costs for instrumentation, energy and precursors are far less for Hydrothermal method. *Lead Tungstates synthesized at room temperature by Hydrothermal method do not contain Schottky defects usually present in similar materials prepared at high temperatures which results in improved luminescent properties.* This facile method does not need any seed, catalyst, harmful and expensive surfactant or template thus it is promising for large-scale and low-cost production with high-quality  $\text{PbWO}_4$  nanophosphor with various morphologies.

## Applications

On passing current through low-pressure Hg discharge, UV light having wavelength 254 nm is generated. This light is invisible and harmful and has to be converted into visible light. This can be done by the application of  $\text{PbWO}_4$  spherical hollow nanoparticles (HNPs) which are produced at 125°C temperature because they show strong absorption at 254 nm and convert this into visible light very efficiently. Cerium doped  $\text{PbWO}_4$  can be used for *green emitting Lamp phosphor*. The application of Oxidic inorganic nano particles doped by lanthanides is thus an Interesting alternative to the use of organic fluorophores and quantum dots for many application areas, e.g., in medical diagnostics, in biological sensors, and in fluorescence marking of biological probes for high throughput screening. Hollow Nano tubes of  $\text{PbWO}_4$  can be

used or *nano fluidic application* in biomedical science. Early up-conversion lasers were demonstrated with bulk crystals, which often had to be cooled to very low temperatures, making the systems impractical. Nowadays, most *up-conversion lasers* are based on nano fibers, where high pump intensities can be maintained over long lengths, so that the laser threshold can be reached even under otherwise difficult conditions. 1-dimensional HNTs shows strong up-conversion at 625 nm wavelength which can be used for such application. Though our assumptions are primitive further research required for practical application of  $\text{PbWO}_4$  nano phosphor in above proposed areas.

#### **Future Work**

Our future planning is to prepare  $\text{PbWO}_4$  using  $\text{PbCl}_2$  with different Cerium concentration and do optimization of its Photoluminescence intensity.

## RESEARCH OUTPUT

### In Journals

1. *Effect of Lead source and Cerium(III) doping on structural and photoluminescence properties of PbWO<sub>4</sub> microcrystallites synthesized by hydrothermal method*,  
**D. Tawde**, M. Srinivas and K. V. R. Murthy, Phys. Status Solidi A, Vol.208, Issue 4, page 803- 807, 2011.
2. *Effect of Temperature and Doping of Cerium on PbWO<sub>4</sub> nano Phosphor*,  
**D.Tawde**, Dhaval Modi, M.Srinivas and K.V.R. Murthy, manuscript accepted to be published in International Journal of Luminescence and its Applications, 2012.

### In Conference Proceedings

1. *Optical and Structural characterization of rare earth doped PbWO<sub>4</sub> nanocrystallites*,  
**D.Tawde**, Dhaval Modi, M.Srinivas, K.V.R.Murthy, Proceedings of 1<sup>st</sup> National Conference On Recent Trends of Physics in Technology & Life Sciences August 19, 2011, Indore
2. *Hydrothermal preparation and Photoluminescence of bundle-like structure of CdWO<sub>4</sub> nanorods*,  
Dhaval Modi, **D. Tawde** and M. Srinivas, UGC Sponsored Seminar on Current Trend in Physics and its Applications, 5Jan, 2011, Dabhoi.
3. *Structural , Dielectric and Optical characterization of Pb<sub>0.3</sub>(Zn<sub>0.35</sub>W<sub>0.35</sub>)O<sub>3</sub>*  
Dhaval Modi, **D. Tawde** and M. Srinivas, 54<sup>th</sup> Proceeding of DAE-SSPS, 869-870(2009), The M.S.University of Baroda.
4. *Structural and Optical study of PbWO<sub>4</sub> nano crystals prepared by Micro-emulsion Hydrothermal method*  
**D.Tawde**, M. Srinivas and Sunil Shah, 54<sup>th</sup> Proceeding of DAE-SSPS,337-338 (2009), The M.S.University of Baroda.
5. *Photoluminescence of PbWO<sub>4</sub> Nanocrystallites Using Hydrothermal Preparation*.  
**D. Tawde** and M. Srinivas, Proceedings of the National Conference on Luminescence and its Application, 24-25 (2009), Kolkata.
6. *Structural , Optical and Dielectric properties of (Pb,Sr)WO<sub>3</sub>*,  
**D.Tawde** and M.Srinivas, 53<sup>rd</sup> Proceeding of DAE-SSPS, 211-212(2008) at BARC.

# Effect of lead source and cerium (III) doping on structural and photoluminescence properties of $\text{PbWO}_4$ microcrystallites synthesized by hydrothermal method

D. Tawde<sup>\*1</sup>, M. Srinivas<sup>1</sup>, and K. V. R. Murthy<sup>2</sup>

<sup>1</sup> Faculty of Science, Physics Department, The Maharaja Sayajirao University of Baroda, Vadodara-390002, Gujarat, India

<sup>2</sup> Faculty of Technology and Engineering, Applied Physics Department, The Maharaja Sayajirao University of Baroda, Vadodara-390001, Gujarat, India

Received 13 September 2010, revised 24 November 2010, accepted 20 December 2010

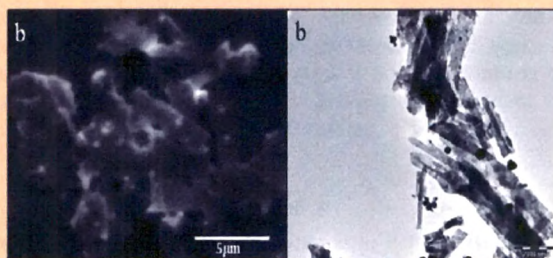
Published online 19 January 2011

**Keywords** doping, electron microscopy, hydrothermal synthesis,  $\text{PbWO}_4$ , photoluminescence, X-ray diffraction

\* Corresponding author: e-mail [dharmendra\\_tawde@yahoo.com](mailto:dharmendra_tawde@yahoo.com), Phone: +91 99 242 60 739/0265-2795339, Fax: 0265-2795569  
Web: [www.msubaroda.ac.in](http://www.msubaroda.ac.in)

Microcrystalline undoped as well as cerium-doped lead tungstate ( $\text{PbWO}_4$ ) powder with different phase and shape, were successfully synthesized via a low-temperature hydrothermal method using different lead sources (lead acetate and lead nitrate) and  $\text{Na}_2\text{WO}_4$  as metallic cations and distilled water as solvent. The effect of lead sources and  $\text{Ce}^{3+}$  doping on crystallite size and shape were investigated with XRD, SEM and TEM. The average crystallite size was found between 28 and 82 nm using the Scherrer formula. Incorporation of  $\text{Ce}^{3+}$  into undoped  $\text{PbWO}_4$  reduces the average crystallite size. The raspite phase of  $\text{PbWO}_4$  generates nanobelts-like structure. Photoluminescence spectra show broad blue–green emission in the 450–550 nm range and the luminescence intensity decreases

with cerium doping compared to undoped  $\text{PbWO}_4$  due to the nonradiative  $5d-4f$  transition of the excited  $\text{Ce}^{3+}$ .



© 2011 WILEY-VCH Verlag GmbH & Co. KGaA, Weinheim

**1 Introduction** The shape- and size-controlled synthesis of inorganic materials at all dimensions from nanoscale to macroscale is a challenging issue to material scientists [1–8] because these could determine the optical, electronic and magnetic properties of the materials and also the performances of those material-based devices [9–13]. Most of the previous approaches for the preparation of  $\text{PbWO}_4$  required high temperature and harsh reaction conditions, such as a high-temperature solid-state reaction for powders [14, 15]. Lead tungstate thin films have been prepared by various metal oxide thin films with  $\text{WO}_3$  vapor [16] and single crystals have been grown from the melt using the methods of Czochralski [17, 18] and Bridgman [19]. However, few studies on the synthesis and luminescent

properties of nano-sized  $\text{PbWO}_4$  powders prepared via the hydrothermal method have been reported [20, 21].

In the present work, we report the synthesis of undoped as well as cerium-doped  $\text{PbWO}_4$  microcrystallites using the hydrothermal method. We have studied the effect of different lead sources and cerium doping on structural, particle morphology and luminescence properties of as synthesized  $\text{PbWO}_4$  powder that were characterized by XRD, SEM, TEM and photoluminescence (PL).

## 2 Experimental

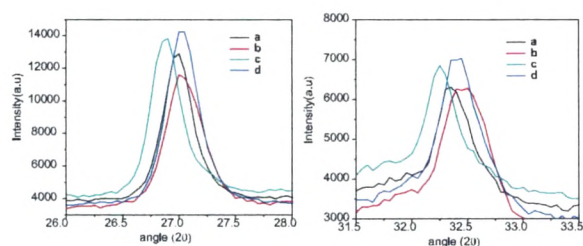
**2.1 Sample preparation** Lead sources [lead acetate [ $\text{Pb}(\text{CH}_3\text{COO})_2$ ], lead nitrate [ $\text{Pb}(\text{NO}_3)_2$ ]],  $\text{Na}_2\text{WO}_4 \cdot 2\text{H}_2\text{O}$  and  $\text{CeO}_2$  purchased from Alfa Aesar were all A.R. grade

© 2011 WILEY-VCH Verlag GmbH & Co. KGaA, Weinheim



**Table 1** Summary of produced phase, lattice parameters and average crystallite size calculated using Scherrer formula for undoped and cerium-doped  $\text{PbWO}_4$  samples.

sample	JCPDS card No.	phase	cell parameter (nm)			average crystallite size (Scherrer formula) nm
			<i>a</i>	<i>b</i>	<i>c</i>	
a	01-070-7590	stolzite	5.4697	5.4698	12.063	38.53
b	00-019-0708	stolzite	5.4619	5.4619	12.049	28.05
	00-016-0156	raspite	13.525	4.9682	5.546	
c	00-008-0476	stolzite	5.4616	5.4616	12.046	82.90
d	00-008-0476	stolzite	5.4616	5.4616	12.046	26.03

**Figure 3** (online colour at: [www.pss-a.com](http://www.pss-a.com)) Magnified XRD spectrum of two characteristic peaks of  $\text{PbWO}_4$ . (a) Magnified (112)  $2\theta$  diffraction peak between 26 and  $28^\circ$ . (b) Magnified (200)  $2\theta$  diffraction peak between 31.5 and  $33.5^\circ$ .

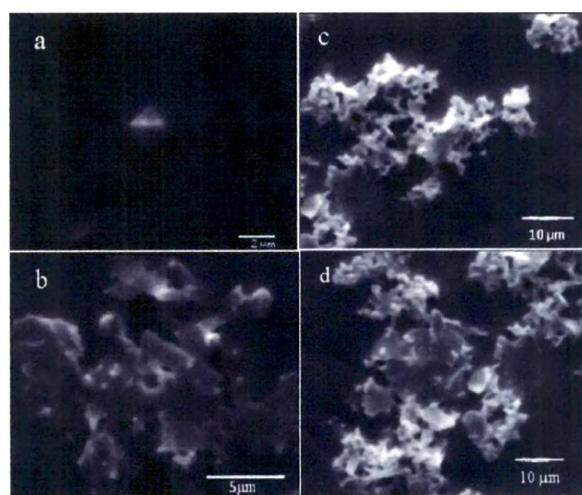
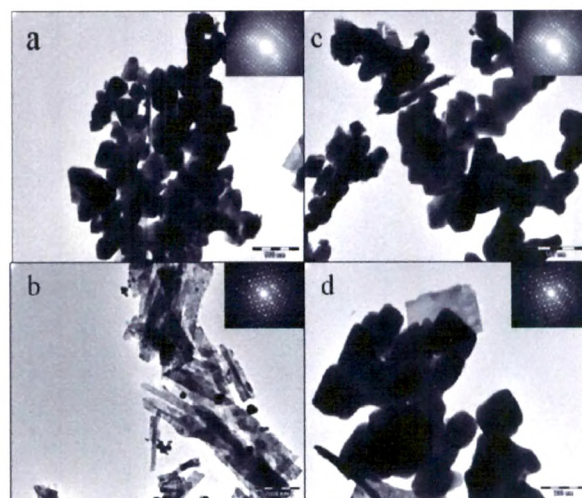
conclusion that the decrease in size of crystallites is occurring due to cerium doping. The substitution of  $\text{Ce}^{3+}$  ion with ionic radius (0.103 nm) is slightly smaller than that of  $\text{Pb}^{2+}$  (0.120 nm) [22] which could be the possible reason for the occurrence of this interesting phenomenon.

**3.2 SEM** The morphological studies of undoped and cerium-doped  $\text{PbWO}_4$  samples were characterized with field effect scanning electron microscopy (FESEM) is shown in Fig. 4a–d. SEM images reveal that as-prepared samples are of micrometer size.

From Fig. 4a it is observed that hydrothermally prepared  $\text{PbWO}_4$  microcrystals are bipyramidal octahedral shaped. Figure 4b shows the nanobelt-like structure of sample b with a few nm thickness. In Fig. 4c coagulation of such microcrystals is observed. From Fig. 4d, some plate-like structure is seen between coagulated microcrystals. Nanobelt-like structure is produced due to raspite phase of  $\text{PbWO}_4$ . A similar effect is also seen in Fig. 4d but in smaller proportion. Hence, from SEM images it is concluded that raspite phase of  $\text{PbWO}_4$  generates nanobelts-like structure.

**3.3 TEM** The morphologies and macrostructures of the as-prepared samples were further investigated by TEM and electron diffraction patterns (EDP) of the  $\text{PbWO}_4$  microcrystallites prepared by the hydrothermal method at  $100^\circ\text{C}$ .

Figure 5a and c indicate that the obtained samples were a mixture of  $\text{PbWO}_4$  nano- and microcrystals with rhombic and spindle-shape, while Fig. 5b shows 1D nanobelts and

**Figure 4** SEM images of undoped and cerium-doped  $\text{PbWO}_4$  samples; (a) sample a, (b) sample b, (c) sample c, (d) sample d.**Figure 5** TEM images of undoped and cerium-doped  $\text{PbWO}_4$  samples; (a) sample a, (b) sample b, (c) sample c, (d) sample d.



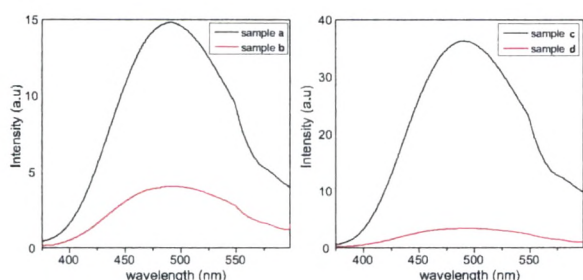


**Figure 6** (online colour at: [www.pss-a.com](http://www.pss-a.com)) Room-temperature PL spectra when (a)  $\text{Pb}(\text{CH}_3\text{COO})_2$  is used as a lead (Pb) source and (b)  $\text{Pb}(\text{NO}_3)_2$  is used as a lead (Pb) source.

some plate-like structure is present in between microcrystals, which can be seen from Fig. 5d. The TEM results also support our previous assumption that nanobelts were produced in raspite phase.

**3.4 Photoluminescence (PL) studies** The PL spectra of undoped samples (samples a and c) and cerium-doped samples (samples b and d) of  $\text{PbWO}_4$  are shown in Fig. 6a and b. The PL spectra of undoped and cerium-doped  $\text{PbWO}_4$  were investigated at room temperature using a 305-nm excitation wavelength.

The PL spectra shows broad luminescence in the blue and green range. The broad blue–green emission band around 450–550 nm is observed in all four samples which is in good agreement with reported values [20, 23]. It is well known that stolzite  $\text{PbWO}_4$  of the tetragonal scheelite structure generates two emission bands, i.e. the intrinsic ‘blue’ band around 440 nm and the ‘green’ band around 500 nm [24]. A broad blue luminescence peak around 450 nm is observed in all samples which originates from tetragonal  $\text{WO}_4^{2-}$  groups [25]. The cerium-doped samples (samples b and d) show weaker luminescence intensity than that of undoped samples. The reduction in PL intensity is due to the nonradiative  $5d-4f$  transition of the excited  $\text{Ce}^{3+}$ . Therefore  $\text{Ce}^{3+}$  ions could serve as efficient nonradiative traps in  $\text{PbWO}_4$  crystal lattice [26]. The blue emission originates from the tetragonal  $\text{WO}_4^{2-}$  groups, while the origin of the green emission remains controversial [27]. The green emission is assumed to arise from the  $\text{WO}_4^{2-}$  groups located in the crystal regions of the lead-deficient structure [28]. The green emission of undoped crystals was ascribed to the  $\text{WO}_3$  oxygen-deficient complex anion [29–31]. This emission was connected with the inclusions of the raspite structure formed due to the thermal stress appearing in the process of crystal growth [32, 33].  $\text{PbWO}_4\text{:Ce}$  prepared with lead acetate contains more inclusions of raspite phase as compared to  $\text{PbWO}_4\text{:Ce}$  prepared with lead nitrate, which can be confirmed from the intensity of their PL spectra.

**4 Conclusions** In summary, we have successfully demonstrated the synthesis of stolzite-phase microcrystallites of undoped  $\text{PbWO}_4$  and cerium-doped  $\text{PbWO}_4$

nanobelts with raspite phase by the hydrothermal method using different lead sources. A large amount of raspite phase is observed when  $\text{Pb}(\text{CH}_3\text{COO})_2$  is used as a lead source compared to when  $\text{Pb}(\text{NO}_3)_2$  is used as a lead source. Efforts to find the reason for the well-observed raspite phase due to  $\text{Pb}(\text{CH}_3\text{COO})_2$  are underway. The average crystallite size was found to be between 28 and 82 nm using the Scherrer formula. The formation of nanobelts-like structure is due to raspite phase with a crystallite size of 28.05 nm. A broad blue–green emission band around 450–550 nm is observed in all the samples which originates from tetragonal  $\text{WO}_4^{2-}$  groups. Doping with cerium reduces the PL intensity compared to undoped samples grown by different lead sources. It is concluded that  $\text{Ce}^{3+}$  ions could serve as efficient nonradiative traps in  $\text{PbWO}_4$  crystal lattice. The percentage of raspite phase inclusion is responsible for the intensity of green emission in cerium-doped  $\text{PbWO}_4$  microcrystallites.

**Acknowledgements** D. Tawde is thankful to UGC-New Delhi, for awarding a RFSMS fellowship and Dr. N. P. Lalla (UGC-DAE CSR Indore) for TEM characterization to carry out this research work.

## References

- [1] S. Mann and G. A. Ozin, *Nature* **382**, 313 (1996).
- [2] T. S. Ahmadi, Z. L. Wang, T. C. Green, A. Henglein, and M. L. El-Sayed, *Science* **272**, 1924 (1996).
- [3] H. Yang, N. Coombs, and G. A. Ozin, *Nature* **386**, 692 (1997).
- [4] S. Mann, *Angew. Chem. Int. Ed.* **39**, 3392 (2000).
- [5] L. A. Estroff and A. D. Hamilton, *Chem. Mater.* **13**, 3227 (2001).
- [6] Y. G. Sun and Y. N. Xia, *Science* **298**, 2176 (2002).
- [7] J. Y. Lao, J. Y. Huang, Z. D. Wang, and Z. F. Ren, *Nano Lett.* **3**, 235 (2003).
- [8] S. Frank, P. Poncharal, Z. L. Wang, and W. A. De Heer, *Science* **280**, 1744 (1998).
- [9] C. Burda, X. Chen, R. Narayanan, and M. A. El-Sayed, *Chem. Rev.* **105**, 1025 (2005).
- [10] Y. Yin and A. P. Alivisatos, *Nature* **437**, 664 (2005).
- [11] Y. Jun, J. Choi, and J. Cheon, *Angew. Chem. Int. Ed.* **45**, 3414 (2006).
- [12] B. Wiley, Y. Sun, J. Chen, H. Cang, Z.-Y. Li, X. Li, and Y. Xia, *Mater. Res. Bull.* **30**, 356 (2005).
- [13] H. Cölfen, and S. Mann, *Angew. Chem. Int. Ed.* **42**, 2350 (2003).
- [14] G. Blasse and L. H. Brixner, *Chem. Phys. Lett.* **173**, 409 (1990).
- [15] C. An, K. Tang, G. Shen, C. Wang, and Y. Qian, *Mater. Lett.* **57**, 565 (2002).
- [16] S. Nobuhiro, K. Akihiko, and K. Tadayoshi, *Bull. Chem. Soc. Jpn.* **69**, 1241 (1996).
- [17] K. Nitsch, M. Nikl, S. Ganschow, P. Reiche, and R. Uecker, *J. Cryst. Growth* **165**, 163 (1996).
- [18] N. Senguttuvan, P. Mohan, S. M. Babu, and C. Subramanian, *J. Cryst. Growth* **183**, 391 (1998).
- [19] K. Tanji, M. Ishii, Y. Usuki, K. Hara, H. Takano, and A. Senguttuvan, *J. Cryst. Growth* **204**, 505 (1999).

- [20] A. Changhua, T. Kaibin, S. Guozhen, W. Chunrui, and Q. Yitai, *Mater. Lett.* **57**, 565 (2002).
- [21] Z. Wei, S. Xinyu, C. Guozhu, T. Guangru, and S. Sixiu, *Mater. Lett.* **63**, 285 (2009).
- [22] M. Kobayashi, Y. Usuki, M. Ishii, N. Senguttuvan, K. Tanji, M. Chiba, A. Hark, H. Takano, M. Nikl, P. Bohacek, S. Baccaro, A. Cecilia, M. Diemoz, A. Vedda, and M. Martini, *Nucl. Instrum. Methods Phys. Res. A* **465**, 428 (2001).
- [23] G. Wang and G. Wan, *J. Alloys Compd.* **484**, 505 (2009).
- [24] M. Itoh and M. Fujita, *Phys. Rev. B* **62**, 12825 (2000).
- [25] W. Van Loo, *Phys. Status Solidi A* **27**, 565 (1975).
- [26] M. Nikl, V. V. Laguta, and A. Vedda, *Phys. Status Solidi B* **245**, 1701 (2008).
- [27] M. Anicete-Santos, E. Orhan, M. A. M. A. de Maurera, L. G. P. Simões, A. G. Souza, P. S. Pizani, E. R. Leite, J. A. Varela, J. Andrés, A. Beltrán, and E. Longo, *Phys. Rev. B* **75**, 165105 (2007).
- [28] V. Babin, P. Bohacek, A. Krasnikov, M. Nikl, A. Stolovits, and S. Zazubovich, *J. Lumin.* **124**, 113 (2007).
- [29] M. V. Korzhik, V. B. Pavlenko, T. N. Timoschenko, V. A. Katchanov, A. V. Singovskii, A. N. Annenkov, V. A. Ligun, I. M. Solskii, and J.-P. Peigneux, *Phys. Status Solidi A* **154**, 779 (1996).
- [30] A. Annenkov, E. Auffray, M. Korzhik, P. Lecoq, and J.-P. Peigneux, *Phys. Status Solidi A* **170**, 47 (1998).
- [31] M. V. Korzhik, *Zh. Prikl. Spektrosk.* **61**, 83 (1994).
- [32] M. Itoh, D. L. Alov, and M. Fujita, *J. Lumin.* **87**, 1243 (2000).
- [33] D. L. Alov and S. I. Rybchenko, *Mater. Sci. Forum* **239**, 279 (1997).

# Effect of Temperature and Doping of Cerium on PbWO<sub>4</sub> nano Phosphor

D.Tawde<sup>\*1</sup>, Dhaval Modi<sup>1</sup>, M.Srinivas<sup>1</sup>, K.V.R. Murthy<sup>2</sup>

<sup>1</sup>Physics Department, Faculty of Science, The Maharaja Sayajirao University of Baroda, Vadodara-390002, Gujarat, India.

<sup>2</sup>Display Materials Laboratory, Applied Physics Department, Faculty of Technology and Engineering, The M. S. University of Baroda, Vadodara – 390001 India.

<sup>\*</sup>Corresponding author: [dharmendra\\_tawde@yahoo.com](mailto:dharmendra_tawde@yahoo.com)

## Abstract

*In the present work, we have used a new technique called Hydrothermal method to grow pure as well as Cerium doped PbWO<sub>4</sub> nanocrystallites at two different temperatures (100°C and 180°C). As synthesized material were characterized with different methods like XRD (X-ray diffraction), SEM (Scanning Electron Microscopy), TEM (Transmission Electron Microscopy) and PL (Photoluminescence) at room temperature. XRD studies reveals that as prepared samples are polycrystalline in nature having tetragonal scheelite (stolzite) phase with space group I4<sub>1</sub>/a and monoclinic raspite (wolframite) phase with P2<sub>1</sub>/c space group. Broad blue emission arises from the WO<sub>4</sub><sup>2-</sup> related tightly bounded Frenkel exciton states in the regular PbWO<sub>4</sub> structure. PbWO<sub>4</sub> contains two green emission bands at room temperature. One is produced due to WO<sub>4</sub><sup>2-</sup> lead deficient scheelite type PbWO<sub>4</sub> while other is due to WO<sub>3</sub> oxygen vacancies of the type of WO<sub>3</sub> complex. By doping trivalent rare earth ion Ce<sup>3+</sup> green emission decreases due to suppression of the oxygen vacancies. With increase in temperature emission bands become gradually shifted to lower energies.*

**Keywords:** Hydrothermal method, X-ray diffraction, Photoluminescence, Scintillation detector

## 1.0 INTRODUCTION

Controlled variation in shape and size of inorganic nano- and micro- materials are important factor that determine their electrical and optical properties. Controlling the architecture and morphology of materials at all dimensions is a challenging issue to material scientists[1-5].

PbWO<sub>4</sub> is a quite unique phosphor material because it possess two stable structure modifications under normal conditions. PbWO<sub>4</sub> phosphor is most attractive for high-energy physics applications because of its high density (8.3 g/cm<sup>3</sup>), short decay time (less than 10 ns), and high-irradiation damage resistance (10<sup>7</sup> rad for undoped and 10<sup>8</sup> rad for La-doped PbWO<sub>4</sub>). Trivalent rare earth ion doped PbWO<sub>4</sub> single crystals are also used in Microwave, Optical fiber, Scintillator material, Humidity sensor, Catalysis, etc[6-9].

## 2.0 EXPERIMENTAL

Pb(CH<sub>3</sub>COO)<sub>2</sub>, Na<sub>2</sub>WO<sub>4</sub>·2H<sub>2</sub>O and CeO<sub>2</sub> purchased from Alfa Aesar were all are A.R.(analytical reagent) grade purity and used without further purification. Distilled water was used to prepare all required solutions. Initially 30 ml solution of 0.01 M concentration of Pb(CH<sub>3</sub>COO)<sub>2</sub> was prepared by continuous stirring and 30 ml solution of 0.01 M concentration of Na<sub>2</sub>WO<sub>4</sub> concentration was added in it. Three samples were prepared in this way are called sample **a**, **b** and **c**. 0.001 M concentration of CeO<sub>2</sub> was added into sample **c**. These three solutions were transferred to Teflon lined stainless steel autoclave of 90 ml capacity filled 80%

with reaction media (i.e.distilled water) one by one in three separate experiments. The autoclave was maintained at temperature 180°C for sample **a** and at 100°C for sample **b** and **c** for 12 hr respectively and then air cooled to room temperature. Obtained precipitates were washed several times with distilled water and lastly with absolute ethanol. Finally white powder was obtained after drying in vacuum at 80°C for 2hr.

## 3.0 CHARACTERIZATION

Powder X-ray diffraction (XRD) patterns were recorded with a Japan Rigaku D/max-RB diffractometer at a scanning rate of 3°/min using Cu K $\alpha$  radiation ( $\lambda$ = 0.15406 nm). Morphology of as-prepared samples were studied with JEOL JSM-6380LV scanning electron microscopy (FESEM). The microstructure and surface morphology of the microcrystalline powders were observed by transmission electron microscopy (TEM, Tecnai 20 G2 FEI made). The photoluminescence (PL) of these samples were investigated on a Shimadzu spectrofluorophotometer at room temperature with Xenon lamp as excitation source.

## 4.0 RESULTS AND DISCUSSIONS

### 4.1 X-ray diffraction (XRD)

Fig. 1 shows the typical XRD patterns of undoped PbWO<sub>4</sub> (sample **a** and sample **b**) synthesized at 100° C and 180° C respectively and cerium doped PbWO<sub>4</sub> (sample **c**)



synthesized at 100° C. Primitive xrd patterns were refined with PowderX software (provided by Cheng Dong) and Cu

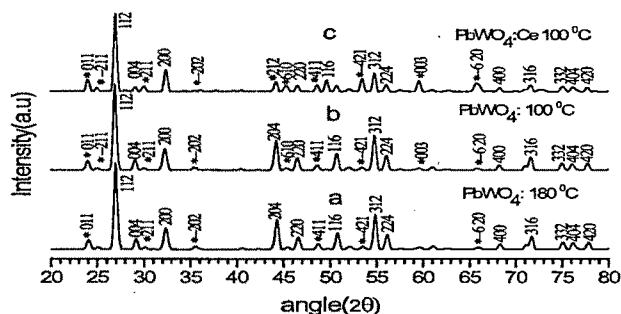


Fig.1: Xrd of  $\text{PbWO}_4$

$K\alpha_2$  removal, background subtraction, adaptive smoothing were done. All diffraction peaks are indexed to a tetragonal stolzite (stolzite) phase with cell parameters  $a = 5.46\text{\AA}$  and  $c = 12.06\text{\AA}$  (JCPDS Card Number 08-0476) and  $a = 13.52\text{\AA}$ ,  $b = 4.9682$  and  $c = 5.54\text{\AA}$  (JCPDS Card Number 00-016-0156) monoclinic (raspite) phase for samples a, b and c respectively. The identification of raspite phase peaks for all samples are marked with symbol (\*).

To observe the effect of temperature on as synthesized undoped  $\text{PbWO}_4$  nanocrystals, xrd patterns of sample a and b were compared. It is cleared from the graph that with increase in temperature crystallinity of prepared samples also increases. As we can see from the graph, some peaks representing raspite phase also present at 180°C but their numbers are less compared to number of peaks at 100°C. Increase in crystallinity and decreases in raspite phase with increase in temperature can be observed from SEM and TEM analysis also which we can see further.

By comparing undoped  $\text{PbWO}_4$  and Ce doped  $\text{PbWO}_4$  (i.e. sample b and sample c), it is observed that intensity of those peaks which represent stolzite phase (i.e. peaks without symbol \*) decreases in sample c and intensity of those peaks which represents raspite phase (i.e. peaks with symbol \*) increases in sample c. From this observation, we can say that undoped  $\text{PbWO}_4$  (sample b) contains less concentration of raspite phase and by doping of cerium, percentage of raspite phase is increased and stolzite phase is decreased [10]. One more observation, which is common to all patterns is that broaden of xrd peaks which represents the decrease in crystallite size of  $\text{PbWO}_4$  compared with large single crystals of  $\text{PbWO}_4$ , there for as prepared samples falls in the range of nanophosphor.

#### 4.2 Scanning Electron Microscopy (SEM)

The morphological analysis of undoped and cerium doped  $\text{PbWO}_4$  nanophosphor was characterized with field effect scanning electron microscopy (FESEM), is shown in figure 2 (a-c). It is observed from the SEM photographs of sample a (fig.2. (a)) and sample b (fig.2. (b)) that hydrothermally

prepared  $\text{PbWO}_4$  nanocrystals are bipyramidal octahedral shaped. In Fig.2 (a) coagulation of such nanocrystals is observed. Fig.2(b) represent an isolated crystal of

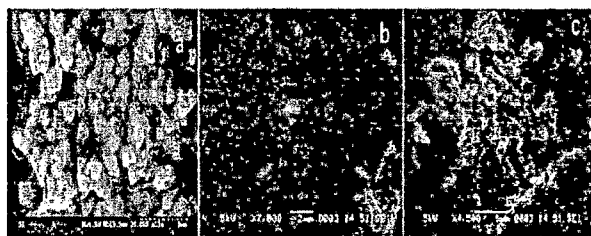


Fig.2: SEM images of  $\text{PbWO}_4$

$\text{PbWO}_4$  with some flake like inclusions. Fig.2(c) shows nanobelt like structure of sample c with few nm thickness and  $\mu\text{m}$  in length. These nanobelts are generated due to raspite phase of  $\text{PbWO}_4$ , which is confirmed from the xrd graphs. Hence we can say that at 100°C temperature bipyramidal octahedral shaped nanocrystals of stolzite phase are formed with some flake like inclusions but at 180°C temperature this flake like inclusions are vanished. On the other hand at 100°C one dimensional growth of nanobelt like structure with raspite phase is accelerated due to cerium doping.

#### 4.3 Transmission Electron Microscopy (TEM)

The morphologies and structure of as-prepared samples were further investigated by TEM as shown in figure 3 (a-b) Figure 3 (a) and Figure 3 (b) denote  $\text{PbWO}_4$  nanocrystals prepared at 180°C and 100°C respectively.

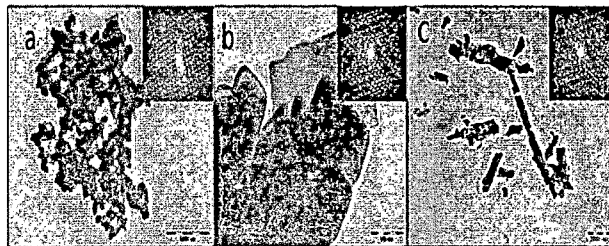


Fig.3: TEM images of  $\text{PbWO}_4$

Scale: (a) 1000 nm (b) 100 nm (c) 2000 nm

Fig. 3 (c) shows cerium doped  $\text{PbWO}_4$  nanorods. Similar to SEM results, TEM images also shows coagulations of  $\text{PbWO}_4$  nanocrystals having diameter less than 100 nm (fig 3(a)) and presence of flake like inclusions of raspite phase (fig 3(b)). One dimensional nanobelt has approximately  $2\mu\text{m}$  in length and 50-60 nm in width which can be confirmed from fig.3(c) [7, 8].

#### 4.4 Photoluminescence (PL)

The room temperature Photoluminescence spectra of  $\text{PbWO}_4$  nanocrystals and Cerium doped  $\text{PbWO}_4$  nanoflakes prepared at two different temperatures (180°C for sample a, 100°C for sample b and sample c) are shown in fig.4. This PL spectrum was recorded at room temperature by using

305 nm excitation wavelength. Primary investigation of PL spectra shows broad emission around 450 nm to 550 nm (blue-green region) of visible band [11, 12], which is the characteristic feature of tungstate family. If we compare PL spectra of sample a with sample b, it is seen that large reduction in PL intensity with decrease in temperature from 180°C to 100°C which remains continue with Ce doping (sample c).

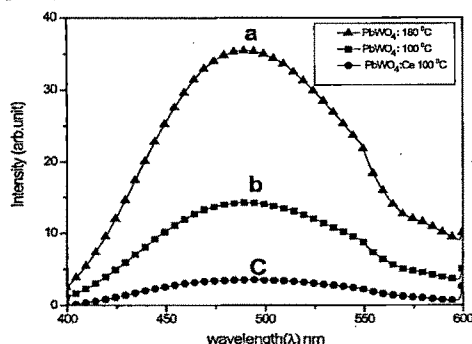


Fig.3: PL spectra of PbWO<sub>4</sub>

Absorption of ultraviolet irradiation occurs by the luminescent tungstate group in PbWO<sub>4</sub> host lattice (sample a and sample b) and by luminescent center Ce<sup>3+</sup> (in sample c). Ultraviolet irradiation is absorbed in PbWO<sub>4</sub> by WO<sub>4</sub><sup>2-</sup> group, and in the excited state of WO<sub>4</sub><sup>2-</sup> group the hole (on oxygen) and the electron (on tungsten) remain together to form a Frenkel exciton, due to strong interaction between them which prevents delocalization hole and electron. Broad emission band in all three spectra suggests the large configurational coordinate ( $\Delta R$ ) change and hence larger the Stokes shift. PL spectra also contain two green emission bands at room temperature. One is produced due to WO<sub>4</sub><sup>2-</sup> lead deficient scheelite type PbWO<sub>4</sub> while other is due to WO<sub>3</sub> oxygen vacancy. As we can see from PL spectra of sample a and sample b that PbWO<sub>4</sub> nanophosphor prepared at 180°C gives high luminescent intensity compared to sample prepared at 100°C at the same position. Luminescence characteristic is connected with morphologies and size of PbWO<sub>4</sub> nanostructures. PbWO<sub>4</sub> nanocrystals prepared at 180°C (sample a) contains high percentage of tetragonal stolzite phase as compared to sample b (can be observed from XRD (fig.1), SEM (fig.2) and TEM (fig.3)) and also contains less amount of structural imperfection which might lead to higher luminescence intensity. Large amount of luminescence intensity suppression in sample c can be attributed due to cerium doping followed by formation of raspate phase. The Ce<sup>3+</sup> ion has ground state configuration 4f<sup>1</sup> and excited state configuration 5d<sup>1</sup>. The 4f<sup>1</sup> state yields two levels (i.e. <sup>2</sup>F<sub>5/2</sub> and <sup>2</sup>F<sub>7/2</sub>) due to spin-orbit coupling and The 5d<sup>1</sup> state split into 2 to 5 levels by the crystal field. These crystal field components which are present in the band gap of PbWO<sub>4</sub> nanophosphor crystal lattice results nonradiative

return of absorbed energy by forming efficient nonradiative traps[12].

## 5.0 CONCLUSIONS

Polycrystalline PbWO<sub>4</sub> nanophosphor with tetragonal stolzite phase formed at 180°C and 1-Dimensional nanorods with monoclinic raspate phase are generated due to doping of cerium at 100°C. PbWO<sub>4</sub> nanocrystals having dimensions less than 100 nm and PbWO<sub>4</sub> nanobelts around 2μm in length and 50-60 nm in width. PL spectrum shows broad emission around 450 nm to 550 nm in blue-green region. Luminescence intensity is suppressed with decrease in temperature attributed due to cerium doping followed by formation of raspate phase. Ce<sup>3+</sup> is also strongly decreases green emission due to suppression of oxygen vacancies. Thus we can conclude that Temperature and Cerium plays an important role to synthesize PbWO<sub>4</sub> nanophosphor with different morphologies and these factors are also effect on optical properties which can be helpful in many applications.

## ACKNOWLEDGMENTS

D.Tawde is thankful to UGC-New Delhi, for awarding RFSMS fellowship, Dr.N.P.Lalla (UGC-CSR, Indore Center) for TEM characterization to carry out research work presented in this paper.

## References:

1. Z.W.Liu, Y. Bando, Adv. Mater.15, 2003, 303
2. W.Z.Wang, G.H.Wang, X.S.Wang, Y.J. Zhan,Y.K. Liu,Adv. Mater.14,2002, 67
3. Y.Feldman, E.Wasserman, D.J.Srolovita, R.Tenne Science,267,1995, 222
4. M.H.Huang, Y.Wu, H.Feick, N.Tran, E.Weber, P. Yang, Adv. Mater,13,2001,113
5. Z.W.Pan, Z.R.Dai, Z.L.Wang, Science, 291, 2001, 194.
6. Y.L.Huang, H.J.Seo, W.L.Zhu, Phys.Status Solidi a, 201,2004, 85
7. X.L.Hu,Y.J.Zhu, Langmuir,20,2004,1521
8. C.S.Shi,Y.G.Wei, X.Y.Yang, D.F.Zhou, C.X.Guo, J.Y.Liao, H.G.Tang, Chem. Phys. Lett., 328,2000,1
9. J.Geng, J.J.Zhu, H.Y.Chen, Cryst. Growth. Des. 6,2006, 321
10. D.Tawde,M.Srinivas, K.V.R.Murthy, Phy.Stat.Sol.a, 208, 2011, 803-807.
11. W. Van Loo, Phys. Stat. Solidi a 27,1975,565.
12. M. Nikl, V. V. Laguta, A. Vedda, Phys. Stat. Solidi b 245, 2008,1701.

# Optical And Structural Characterization Of Rare Earth Doped PbWO<sub>4</sub> Nanocrystallites

D.Tawde<sup>1†</sup>, Dhaval Modi<sup>1</sup>, M.Srinivas<sup>1</sup>, K.V.R.Murthy<sup>2</sup>

<sup>1</sup> Physics Department, Faculty of Science, The M.S. University of Baroda, Vadodara, Gujarat, India.

<sup>†</sup>dharmendra\_tawde@yahoo.com

<sup>2</sup> Applide Physics department, Faculty of Technology and Engineering, The M.S. University of Baroda, Vadodara, Gujarat, India.

## Abstract

Nano sized Lead Tungstate (PbWO<sub>4</sub>) crystallites were successfully synthesized via hydrothermal method using distilled water as reaction media. The effect Lead Chloride as a base material and the doping of rare earth ion Ce<sup>3+</sup> on the structure formation of PbWO<sub>4</sub> and its optical properties have been investigated. The morphologies of as prepared samples were characterized using Field Effect Scanning electron microscopy (FESEM) and phase identification was conducted by the X-ray diffraction (XRD). The examination of Photoluminescence (PL) properties of as-prepared samples revealed that the intensity of emission of PbWO<sub>4</sub> nanocrystallites strongly depend on preparation conditions. Two emission bands of PbWO<sub>4</sub> are wellknown i.e. the intrinsic blue band in the range 400-450 nm and the green band in the range 500-550 nm. The emission spectra in blue range are occurring due to radiative transition of [WO<sub>4</sub><sup>2-</sup>] complex. It is observed from our measurements that doping of Ce<sup>3+</sup> decrease the Photoluminescence intensity suggest that Ce<sup>3+</sup> perform role of non radiative trap.

**Key Words:** Photoluminescence, XRD, SEM, Hydrothermal method.

## 1. Introduction

The development of a wide range of nanomaterials has sparked tremendous interest on account of their novel physical properties and their potential applications in constructing electronic and optoelectronic devices at the nanoscale, so controlling the architecture and morphology of materials at all dimensions is a challenging issue to material scientists [1-4]. PbWO<sub>4</sub> is most attractive for high-energy physics applications because of its high density (8.3 g/cm<sup>3</sup>), short decay time

(less than 10 ns), and high-irradiation damage resistance (10<sup>7</sup> rad for undoped and 10<sup>8</sup> rad for La-doped PbWO<sub>4</sub>) [5-8].

In the present work, we have used hydrothermal method to grow pure and Cerium doped PbWO<sub>4</sub> microcrystallites at low temperature. We have studied the effect of lead source (PbCl<sub>2</sub>) as well as roll of Cerium in synthesized PbWO<sub>4</sub>: Ce and characterization is done by XRD, SEM and PL.

## 2. Experimental

PbCl<sub>2</sub>, Na<sub>2</sub>WO<sub>4</sub>·2H<sub>2</sub>O and CeO<sub>2</sub> purchased from Alfa Aesar were all A.R. grade purity and used without further purification. Distilled water was used to prepare all the required solutions. Initially 30 ml solution of 0.01 M concentration of lead source PbCl<sub>2</sub> was prepared by continuous stirring and 30 ml solution of 0.01 M concentration of Na<sub>2</sub>WO<sub>4</sub> concentration was added in it. Some amount of these solutions was collected in different beakers in which 0.001 M concentration of CeO<sub>2</sub> was added. The prepared two solutions were transferred to Teflon lined stainless steel autoclave of 90 ml capacity filled with reaction media of 80% one by one. The autoclave was maintained at a temperature of 150°C for both samples for 12 hrs and air cooled to room temperature. Obtained precipitates were washed several times with distilled water and lastly with absolute ethanol. Finally white powder was obtained after drying in vacuum at 80°C for 2hrs.

## 3.Characterization

Powder X-ray diffraction (XRD) patterns were recorded with a Japan Rigaku D/max-RB diffractometer at a scanning rate of 3°/min using Cu K $\alpha$  radiation ( $\lambda$ = 0.15406 nm). The microstructure and surface morphology of the microcrystalline powders were studied with JEOL JSM-6380LV scanning electron microscopy

(FESEM). The photoluminescence (PL) of the samples was investigated on a Shimadzu spectrofluorophotometer at room temperature with Xenon lamp as excitation source.

## 4. Structural studies

### 4.1 X-ray diffraction (XRD)

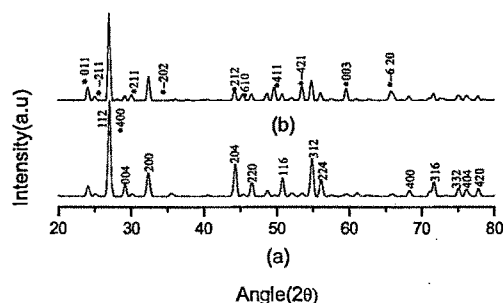


Figure 1 XRD pattern of (a)  $\text{PbWO}_4$  nanocrystals grown with  $\text{PbCl}_2$  (b)  $\text{Ce}^{3+}$  doped  $\text{PbWO}_4$

Fig. 1 shows the typical XRD pattern of as-prepared samples of  $\text{PbWO}_4$  sample. All diffraction peaks are indexed to a tetragonal scheelite (stolzite) phase and monoclinic raspite phase for sample a and b respectively. The identification of raspite phase peaks of sample b are marked with symbol (\*). It is inferred from Fig. 1 that stolzite phase of  $\text{PbWO}_4$  was obtained by using  $\text{PbCl}_2$  as lead sources. Incorporation of cerium into these samples produce raspite phase of  $\text{PbWO}_4$  in small proportion.

### 4.2 Scanning Electron Microscopy (SEM)

The morphological studies of pure and cerium doped  $\text{PbWO}_4$  samples were characterized with Field Effect Scanning Electron Microscopy (FESEM) are shown in Fig.2.

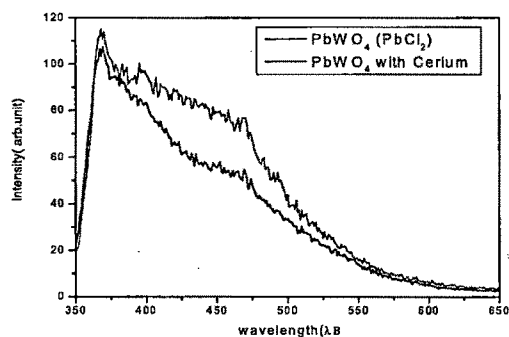


Figure 2 SEM images of (a)  $\text{PbWO}_4$  nanocrystals grown with  $\text{PbCl}_2$  (b)  $\text{Ce}^{3+}$  doped  $\text{PbWO}_4$

From Fig.2 (a) it is observed that hydrothermally prepared  $\text{PbWO}_4$  microcrystals are bipyramidal octahedral shaped. (b) shows nanoflak like structure with few nm thickness.

### 4.3 Photoluminescence (PL)

Fig.4 shows Photoluminescence spectra of  $\text{PbWO}_4$  prepared at different temperatures and with  $\text{Ce}^{3+}$ .  $\text{PbWO}_4$  broad blue band luminescence 400-500 nm which is the characteristic behavior of tungstates. [9,10]. Two emission bands of  $\text{PbWO}_4$  are wellknown i.e. the intrinsic blue band in the range 400-450 nm and the green band in the range 500-550 nm. The emission spectra in blue range are occurring due to radiative transition of  $[\text{WO}_4]^{2-}$  complex. According to photoluminescence spectra intensity decreases with Ce doping.



## Acknowledgments

D.Tawde is thankful to UGC-New Delhi, for awarding RFSMS fellowship, UGC-DRS for providing research facilities, to carry out this research work.

## References

- [1] J.Y. Lao, J.Y. Huang, Z.D. Wang, Z.F. Ren, *Nano Lett.* 2003, pp.3235-3240.
- [2] M. Kobayashi, M. Ishii, Y. Usuki, *Nucl. Instrum. Methods A* 406,1998, pp. 442.
- [3] Y.G. Sun, Y.N. Xia, *Science* 298, 2002, pp.2176.
- [4] C.M. Lieber, *Solid State Commun.* 107, 1998, pp.607-616.
- [5] J. Geng, J.J. Zhu, H.Y. Chen, *Cryst. Growth Des.* 6, 2006, pp.321-326.
- [6] K. Hara, M. Ishii, M. Nikl, H. Takano, M. Tanaka, K. Tanji, Y.Usuki, *Nucl. Instrum. Methods A*, 414, 1998 pp.325.
- [7] GuizhenWang, GengpingWan, *Journal of Alloys and Compounds* 484, 2009, pp.505-509.
- [8] M. Itoh, M. Fujita, *Phys. Rev. B* 62, 2000,pp.12825.
- [9] W. Van Loo, *Phys. Stat. Solidi a* 27, 1975,pp.565.
- [10] M. Nikl, V. V. Laguta, A. Vedda, *Phys. Stat. Solidi b* 245, 2008,1701.



## Structural and Optical study of PbWO<sub>4</sub> nano material prepared by Micro-emulsion hydrothermal method

D.Tawde<sup>†</sup>, M.Srinivas<sup>†</sup> and Sunil Shah<sup>\*</sup>

<sup>†</sup>Department of Physics, Science Faculty,  
The Maharaja Sayajirao University of Baroda, Vadodara, 390002.

<sup>\*</sup>Shah-Schulman Centre for Surface Science and Nanotechnology,  
Dharmsinh Desai University, Nadiad, Gujarat, India 387001

Email: dharmendra\_tawde@yahoo.com

### Abstract

PbWO<sub>4</sub> nano crystals prepared by hydrothermal method using micro emulsion system. As prepared samples are characterized with DLS, SEM, PL, and FTIR. The effective diameter of PbWO<sub>4</sub> nanomaterial obtained from the Stokes-Einstein relation is 96.9 nm. PbWO<sub>4</sub> nano crystals having tetragonal structure were characterized by SEM. We investigated upconversion emission in UV band 360nm under 630 nm excitation and up and down conversion emission in UV and IR band at 300nm and 630nm under 400 nm excitation wavelength respectively. The absorption band around 7000-9000 cm<sup>-1</sup> was ascribed to the W-O stretching vibration in WO<sub>4</sub> tetrahedron.

### INTRODUCTION

The luminescence of lead tungstate (PbWO<sub>4</sub>) was first researched around 40 years ago. Now days it has great technological importance as an inorganic scintillation crystals due to its high density (8.3 g/cm<sup>3</sup>), Short decay time (less than 10 ns) and high irradiation damage resistance (10<sup>7</sup> rad for undoped and 10<sup>8</sup> rad for La-doped PbWO<sub>4</sub>) [1,2]. PbWO<sub>4</sub> has been approved for use in Compact Muon Solenoid (CMS) and Assembly Line Balance (ALICE) experiments to construct a precision electron-magnetic calorimeter at Large Hadron Collider (LHC). Nowadays nanometer-sized inorganic materials have attracted much interest from scientists, due to their wide range of optical and electrical properties [3,4]. In this work, we described a micro emulsion [5,6,7] hydrothermal method to synthesize PbWO<sub>4</sub> nano crystals.

### EXPERIMENTAL

The micro emulsion system was composed of TritonX-100, cyclohexane, water and 1-hexanol. The amounts of each component used in a typical reaction for Wo (water to surfactant molar ratio) of 3 are 8 % Triton X-100, water and 1-hexanol at 0.027 % (v/v) each with cyclohexane as the remainder. Next 2.5 ml Na<sub>2</sub>WO<sub>4</sub> (0.10 M) aqueous solution and 2.5 ml Pb (CH<sub>3</sub>COO)<sub>2</sub> (0.10 M) aqueous solution were separately added to the above ternary system and allowed to stir for 30 minutes under constant stirring at 25 ± 2 °C in separate vial. After getting transparent individual micro-emulsion system mixed both system and allowed to stir for

1 hrs in order to complete reaction. Instantaneous formation of the particles was observed. The resultant micro-emulsion system was then transferred into 125 ml Teflon-lined stainless steel autoclave and heated at 150 °C for 18 hr. The resultant suspension was cooled to room temperature naturally after heating. The sample was collected by centrifugation and washed several times with absolute alcohol and distilled water and dried in vacuum oven.

### CHARACTERIZATION

#### 1. Dynamic Light Scattering

A Brookhaven 90 plus DLS instrument with a solid state laser source operated at 660 nm was used to measure the particle size and size distribution of the prepared micro-emulsion in a dynamic mode. The effective diameter of PbWO<sub>4</sub> obtained from the Stokes-Einstein relation,

$$D = \frac{kT}{3\pi\eta d}$$

is 96.9 nm. Where d is the particle diameter, D is the translational diffusion coefficient, k is Boltzmann constant, T is the temperature (°C), and η is the viscosity of the medium. The scattering intensities from the samples were measured at 90° with a photomultiplier tube. To minimize the inter particle interactions, the analysis of the latex was done after 10 times dilutions with the refractive index and viscosity of cyclohexane considered as that of micro-emulsion. All of the measurements were performed in triplicate.

## 2.SEM



Figure 1 SEM images of PbWO<sub>4</sub> nanocrystals

PbWO<sub>4</sub> nano crystals having tetragonal structure were characterized by SEM as shown in fig.1.[10].

## 3. Photoluminescence

Photoluminescence spectra of PbWO<sub>4</sub> nanocrystals were recorded from OCEAN OPTICS Spectrofluorimeter model HR 2000-CG with different excitation wavelengths at room temperature.

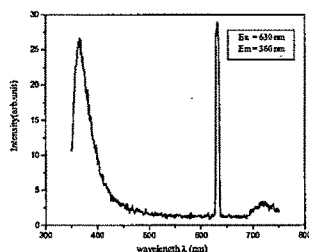


Figure 2(a) PL spectra of PbWO<sub>4</sub> at excitation wavelength 630 nm

The upconversion luminescence spectra of PbWO<sub>4</sub> nanomaterial is investigated as shown in fig.2(a).The photoluminescence upconversion for the UV emission is directly excited with by 630 nm by ground state absorption process (GAS) and/or by energy transfer process. The upconversion is thought due to multiphonon relaxation in the PbWO<sub>4</sub> nanocrystals.

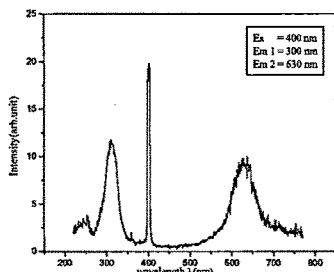


Figure 2(b) PL spectra of PbWO<sub>4</sub> at excitation wavelength 400 nm

The up as well as downconversion spectra is shown in fig. 2(b) under 400nm excitation shows emission bands at 300nm and 630 nm due to stokes and anti-stokes transitions respectively. When nanocrystals are illuminated with light (WO<sub>6</sub>)<sup>6-</sup> anions are excited due to strong absorption of <sup>1</sup>A<sub>1g</sub> → <sup>1</sup>T<sub>1u</sub> transitions [8,9] and then transfer excitation energy to Pb<sup>2+</sup> ions and hence luminescence efficiency is greatly enhanced.

## 4. FTIR

The FTIR spectra of PbWO<sub>4</sub> nanocrystals was recorded by using JASCO Spectrometer FTIR-4100 in the frequency region 350-7800 cm<sup>-1</sup> under a resolution of 4cm<sup>-1</sup> with scanning speed 2mm/sec. The recorded IR spectra were compared with standard spectra of the functional group shown below in fig.2. The absorption band around 7000-9000 cm<sup>-1</sup> was ascribed to the W-O stretching vibration in WO<sub>4</sub> tetrahedron.

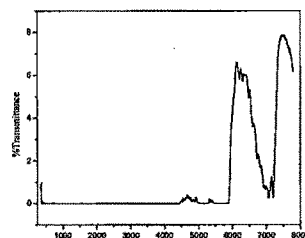


Figure 3: The FTIR spectra of PbWO<sub>4</sub> nanomaterial

## CONCLUSIONS

Present investigation of PbWO<sub>4</sub> nano crystal suggest its use as IR-to-UV convertor, VIS to UV and NIR converter and solid state photonic devices.

## ACKNOWLEDGEMENT

D.Tawde is thankful to Prof. L.M.Manocha and Prof.(Mrs) S. Manocha for providing SEM facility and UGC for an award of RFSMS fellowship for doing research work presented here.

## REFERENCES

1. M. Kobayashi, M. Ishii, Y. Usuki, Nucl. Instrum. Methods A 406 (1998) 442.
2. K. Hara, M. Ishii, M. Nikl, H. Takano, M. Tanaka, et al, Nucl. Instrum. Methods A 414 (1998) 325.
3. G.D. Stucky, J.E. Macdougall, Science 247 (1990) 669.
4. A.P. Alivisatos, Science 271 (1996) 933.
5. Changhua An, Kaibin Tang, Guozhen Shen et al. Materials Letters 57 (2002) 565-568
6. A Pal, Sunil Shah, et al, Colloid Surface A: Physicochemical & Engineering Aspects 337 (2009) 205-207.
7. A Pal, Sunil Shah and S. Devi. Colloids and Surface A: Physicochemical & Engineering Aspects 302 (2007) 483-487.
8. V.O.Sokolov, V.G. Plotnichenko et al, J. Non Cryst. Solids 352(2006)5618.
9. G.Blasse, G.J.Dirkson, Chem.Phys.Letts,85(1982)150.
10. D.Tawde and M.Srinivas in Proceedings of the National Conference on Luminescence and its Applications edited by R. Debnath et al (Kolkatta, 2009) p 24-25.

# PHOTOLUMINESCENCE OF $\text{PbWO}_4$ NANOCRYSTALLITES USING HYDROTHERMAL PREPARATION

D.Tawde\* & M.Srinivas

Physics Department, Faculty of Science, The M.S.University of Baroda, Vadodara-390002,  
Gujarat, India.

Email id: dharmendra\_tawde@yahoo.com

## Abstract

$\text{PbWO}_4$  nanocrystallites were synthesized by hydrothermal technique. The as-synthesized  $\text{PbWO}_4$  nanocrystallites having tetragonal structure were characterized by various techniques: SEM, XRD. The luminescence properties of the  $\text{PbWO}_4$  nanocrystallites were investigated by Photoluminescence (PL) spectroscopy. The PL spectrum for the sample under study exhibits an emission peak in blue- green region.

## Introduction

Recently, controlling the size and dimensionality of nanostructure at the microscopic level is one of the most challenging faced by researchers [1-3]. Low dimensional systems represent one of the important frontiers in advanced material research. Quantum confinement of electrons in low dimensional systems provides a powerful tool for manipulating their optical, electrical and thermo electrical properties [4-6]. Some unique and fascinating properties, such as higher luminescence efficiency, 1D nanostructure have already been demonstrated [7]. Currently, nano stimulated tungstate materials, such as  $\text{CdWO}_4$ ,  $\text{BaWO}_4$ ,  $\text{ZnWO}_4$  [9-15], and so forth, have aroused much interest because of their luminescence behavior, structural properties, and potential applications. The preparation and properties of tungstate materials have received considerable attention. Various techniques have been developed to synthesize tungstate.  $\text{PbWO}_4$  single crystals have also been grown from sodium metasilicate gel using water solutions of lead acetate and sodium tungstate as the reagent [16].

Nanometer-sized inorganic materials have attracted much interest from scientist, due to their wide range of optical and electrical properties [17-19]. In this work, we described a hydrothermal method to synthesize  $\text{PbWO}_4$  nanocrystallites. The as-synthesized samples were investigated at room temperature by means of XRD, SEM and PL.

## Experimental Procedure

Lead acetate  $(\text{CH}_3\text{COO})_2\text{Pb} \cdot 3\text{H}_2\text{O}$  and Sodium tungstate  $\text{Na}_2\text{WO}_4 \cdot 2\text{H}_2\text{O}$  were used of analytical grade purity and distilled water was taken as reaction media. In a typical procedure, 0.1M concentration of Lead acetate and sodium tungstate were added into a Teflon- lined autoclave of 90 ml capacity. Then the autoclave was filled with reaction media up to 80% of its capacity. The autoclave was maintained at temperature 100-120°C for 10 hr and then air cooled to room

temperature. The precipitate was collected, filtered off and washed with distilled water several times and absolute ethanol, successively. After drying in vacuum for 4h, the final white powders were obtained.

### Characterization

The morphologies were characterized using Scanning electron microscopy (SEM). Phase identification was conducted by the X-ray diffraction (XRD) technique, using Cu K $\alpha$  radiation by Rigaku X-ray diffractometer. SEM images were taken with Hitachi S-3000N Scanning electron microscope. The luminescence and excitation spectra of the sample were determined by a Fluorescence spectrometer with Xe lamp at R.T.

### Results and discussion

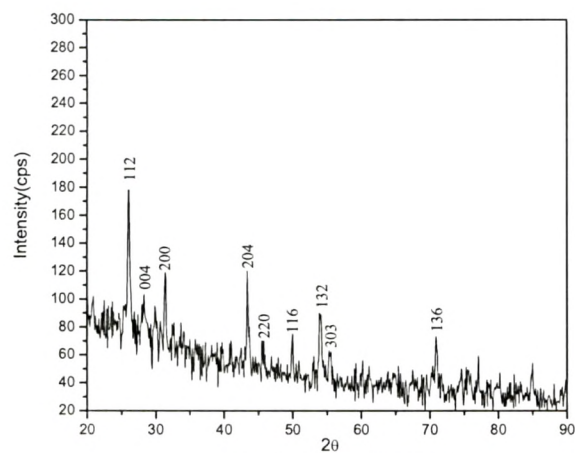


Fig 1 XRD of PbWO $_4$

Fig.1 shows the typical XRD pattern of as-prepared sample grown by using hydrothermal method. All the diffraction peaks are consistent with reported values of (JCPDS Card no.720765).From the XRD it is found that prepared sample consists of Tetragonal system with space group 14 $_1$ /a having lattice parameter a=5.50 and c=12.12.The morphologies of the as-prepared samples by SEM were shown in Fig.2 (a). It could be seen that the sample appeared to show tetragonal structure with diameter 400nm.

It is well known that different tungstate species existed in solution at different pH. A low pH favors the polytungstate species and occurrence of Pb $^{2+}$  ion, while a high pH favors the monotungstate in WO $_4^{2-}$  . Fig 2 show, the SEM images of PbWO $_4$  nanocrystals prepared at a pH of 7 for the formation of nanocrystals when reaction temperature was kept in the range of 100 - 120 °C for 10 h.

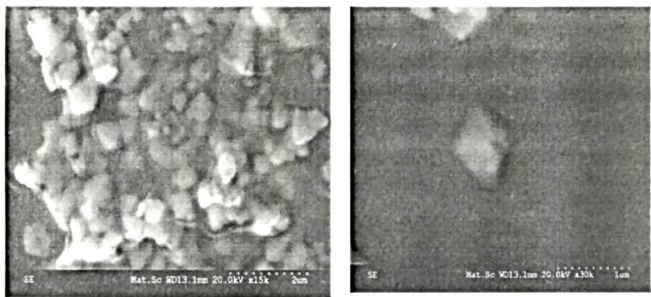


Fig. 2 (a) (b)

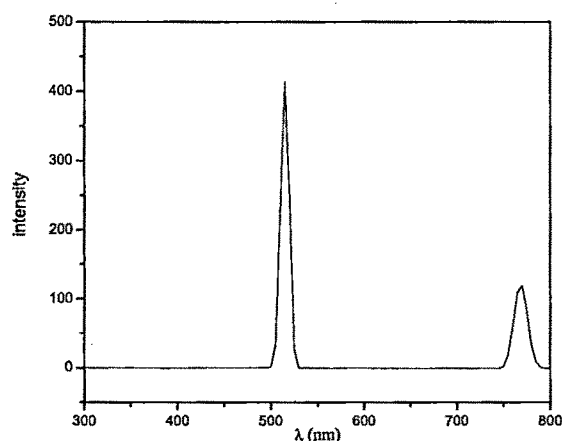


Fig. 3

Fig.3 shows the room temperature PL emissions of  $\text{PbWO}_4$  nanocrystallites hydrothermally prepared. The PL spectrum of sample was measured using a 256 nm excitation line. The spectrum of sample exhibited emission sharp intense peak in blue-green region at 514 nm and weak peak at 768 nm region. The result demonstrated that the morphologies of the nanocrystallites may affect their luminescence characteristics. According to literature, the luminescence properties of  $\text{PbWO}_4$  are very sensitive to the structure and strongly depend on structural defects [20]. Further studies on the mechanism of the PL of  $\text{PbWO}_4$  nanocrystallites are underway.

## Conclusion

In summary,  $\text{PbWO}_4$  nanocrystallites were successfully prepared by via a mild hydrothermal reaction route. Prepared sample consists of Tetragonal system with space group  $4_2/a$  having lattice parameter  $a=5.50\text{nm}$  and  $c=12.12\text{nm}$ . Our examination of the PL property of as-prepared sample revealed that PL of the  $\text{PbWO}_4$  was strongly dependent on structure.

## References

1. R.Jana, L.Gearheart, C.J. Murhpy, *Adv.Mater.*13,1389(2001)
2. Y.G.Sun, Y.N.Xia, *Science* 298,2176(2002)
3. Y.G.Sun, B.Mayers, Y.N.Xia, *Nano Lett.*3,675(2003)
4. J.Rodrigues, K.F.Jensen, H.Mattoussi, I.Michel, B.O.Dabbousi, M.G.Bawendi, *App.Phys.Lett.*70, 2132 (1997)
5. Z.Zhang, D.Gekhtaman, M.S. Dresselhaus, J.Y.Ying, *Chem. Mater.* 11,1659 (1999)
6. L.Pfeiffer, A.Yacoby, H.L. Stormer, K.L. Baldwin, J.Hasen et al., *Microelectron.J.* 28,817(1997)
7. X.Duan, Y.Huang, Y.Cui, J.Wang, C.M.Lieber, *Nature* 409,66 (2001)
8. M. Huang, S.Mao, H. Feick, H. Yan, Y. Wu, H. Kind, E. Weber, R. Russo, P. Yang, *Science* 292,1897(2001)
9. H.W.Liao, Y.F.Wang, X.M. Liu, Y.D.Li, Y.T.Qian, *Chem.Mater.*12,2819(2000)
10. S.H. Yu, M. Antonietti, H.Coffen, M.Giersig, *Angew. Chem.Int.Ed.*41,2356(2002)
11. X.L. Hu, Y.J. Zhu, *Langmuir* 20, 1521(2004)
12. H.T. Shi, L.M. Qi, J.M. Ma, H.M. Cheng, *J. Am. Chem. Soc.* 125, 3450 (2003)
13. S. Kwan, F. Kim, J. Akana, P.D. Yang, *Chem. Commun.*, p.447 (2001).

14. S.J. Chen, J.H. Zhou, X.T. Chen, J. Li, L.H. Li, J.M. Hong, Z.L.Xue, X.Z. You,  
Chem.Phys. Lett. 375, 185 (2003)
15. B. Liu, S.H. Yu, L.J. Li, F. Zhang, Q. Zhang, M. Yoshimura, P.K.Shen, J. Phys. Chem. B  
108, 2788 (2004)
16. K. Tanji, M. Ishii, Y. Usuki, K. Hara, H. Takano, A. Senguttuvan, J. Cryst. Growth 204  
(1999).
17. G.D. Stucky, J.E. Macdougall, Science 247, 669 (1990).
18. A.P. Alivisatos, Science 271, 933 (1996).
19. G. Schmid, Chem. Rev. 92, 1709 (1992).
20. C.S.Shi, Y.G.Wei, X.Y. yang , D.F. Zhou , C.X.Guo, J.Y.Liao, H.G.Tang ,  
Chem.Phys.Lett. 328 ,(2000) 1- 4 .

## Structural, Optical and Dielectric properties of (Pb,Sr)WO<sub>3</sub>

D.Tawde, M.Srinivas

Physics Department, Faculty Of Science, The M.S.University Of Baroda,Vadodara-390002

Email: dharmendra\_tawde@yahoo.com

### Abstract

Polycrystalline PSW ferroelectric ceramics with perovskite structure have been prepared by high temperature solid state reaction technique. Structural analysis with X-ray confirms mixed phases of PWO:SWO solid solution. Thermoluminescence(TL) studies shows high intensity peaks with increase in concentration of Sr<sup>2+</sup> and  $\beta$ -irradiation of high radiation dose. Dielectric studies as a function of dielectric constant( $\epsilon'$ ) and dielectric loss( $\tan \delta$ ) with varying frequency between 100Hz-10MHz in temperature range 25°C-120°C reveals a diffused phase change around 70°C.

### INTRODUCTION

Ferro(seignette)electric ceramics such as PZT,PLZT and PMN etc. are of great interest since last few years due their large applications in electronics and optics. Perovskite solid solutions such as (Ba,Sr)TiO<sub>3</sub> [1] and PLZT [2] shows a diffuse phase transition (DPT) which is identified by broadened  $\epsilon_{\max}$  at Curie point against temperature curve. The electro-optic and optical memory applications of PLZT depends on the amount of substitution of La<sup>3+</sup> in PZT. Based on this idea we reported our effort to enhance optical and electrical properties of PWO perovskite by proper substitution Sr<sup>2+</sup> at A site. As far as our knowledge this is the first attempt to study Thermoluminescence (TL) in term of ferroelectric application. Dielectric properties of PSW ferroelectric has been studied as a function of dielectric constant( $\epsilon'$ ) and dielectric loss( $\tan \delta$ ) with varying frequency between 100Hz-10MHz at different temperature between 25°C-120°C.

### Experimental

All the specimens Pb<sub>1-x</sub>(Sr<sub>x</sub>W<sub>x</sub>)O<sub>3</sub>, where x = 0.5,0.7 used in this investigation were prepared by using PbO, SrCO<sub>3</sub> and WO<sub>3</sub> as starting reactants with high temperature solid state reaction technique. Sample were synthesized from the starting materials of PbO, SrCO<sub>3</sub> and WO<sub>3</sub> in the stoichiometric proportion 0.5: 0.25: 0.25 called Sample1 (S-1) and 0.7: 0.35 : 0.35 called Sample2 (S-2) taken in molar ratio and then mixed thoroughly in agate mortar for 1 hour for each sample and conformed for uniform mixture. The calcination was performed in a closed ceramic crucible at 800°C for 12 h with heating rate of 200°C/h. After calcinations samples are again grinded and then pellets of the size 13.72mm diameter and 1.45 mm thickness are prepared under the pressure of 10 tons. These pellets then sintered at 800°C for 12 h. For better contact surface of pellets as well as electrodes are polished with fine emery

paper and pellets surface are coated with silver. The dielectric properties of the sintered samples are studied with Solartron impedance/Gain-Phase analyzer with changing frequency from 100Hz to 10MHz over the temperature range from RT to 120°C

### Results and Discussion

Figure 1,2 show the X-ray diffraction pattern of PSW samples. It is clear from XRD that both the samples are not single phase but they consist mixed SWO and PWO phases which is tetragonal with space group I4<sub>1</sub>/a in small amount [3].

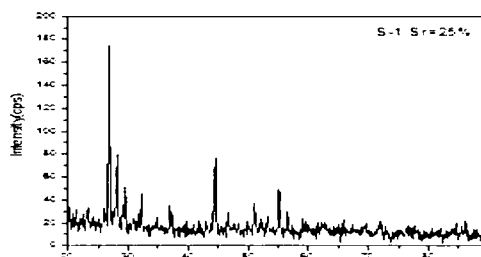


Figure 1 XRD pattern of S-1

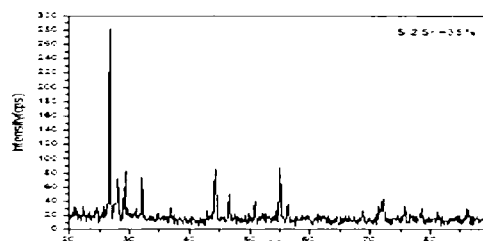


Figure 2 XRD pattern of S-2

Thermoluminescence (TL) experiment was carried out with Nucleonix TL reader. The samples were irradiated

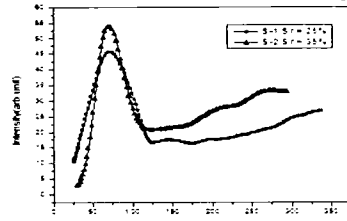


Figure 3 TL curves of S-1 & S-2

from  $\text{Sr}^{90}$   $\beta$ -source with rate 5 Gy/min for 5 minutes. Figure 3 shows TL curve for both  $S_1$  and  $S_2$  samples. It observed that with increase of  $\text{Sr}^{2+}$  concentration a strong glow peak is observed at 75°C. The increase in intensity is attributed due to  $\beta$ -irradiation thereby, results in radiative transitions [6].

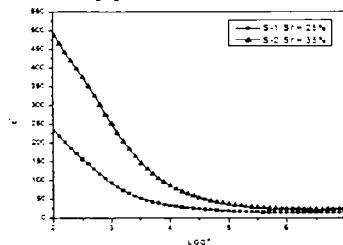


Figure 4 Variation of dielectric constant with frequency

Figure 4 shows strong dependence of dielectric constant on frequency which confirms its relaxor behavior. The dielectric constant increase with increase in concentration of  $\text{Sr}^{2+}$  and decrease with increase in frequency up to 100 kHz and then remains almost constant for remaining frequency. High dielectric constant for  $S_2$  is supposed due to movement multiple domain walls in large grain size of  $S_2$  compared to  $S_1$  with change [4].

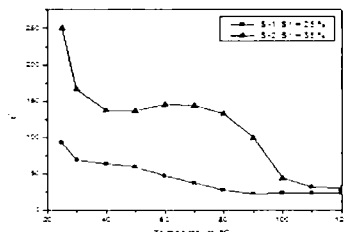


Figure 5 Variation of dielectric constant with temperature at 1KHz

Figure 5 shows that dielectric constant decreases with increase in temperature for both  $S_1$  and  $S_2$  at constant 1kHz frequency but in the case of  $S_2$  it increases at nearby 50°-60°C determines DPT which is suppressed in  $S_1$ . The composition of  $\text{Sr}^{2+}$  and  $\text{Pb}^{2+}$  is selected such a way that it leads to different ferroelectric transition temperature which broadens the dielectric peak. This DPT is due to Phase transition from paraelectric to ferroelectric phase at  $T_c$  [5,7].

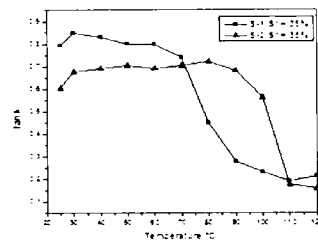


Figure 6 Variation of dielectric loss with temperature at 1KHz

Fig.6 shows the dielectric loss is very less for both the samples it reaches highest value just below Curie point which also satisfied relaxor behavior.

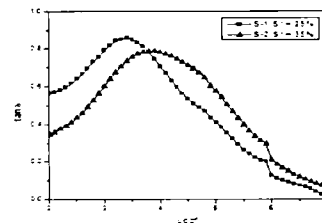


Figure 7 Variation of dielectric loss with frequency

Figure 7 shows variation of dielectric loss with frequency which also very less for both samples. Initially it is increases for both samples reaches maxima at 10kHz but after it decreases with increases in frequency.

## CONCLUSION

The PSW with  $\text{Sr} = 35\%$  shows relaxor ferroelectric phase transition. Among chosen combination of  $\text{Sr}^{2+}$  35% is good for its optical application whereas attempts are made to increase the intensity and dielectric constant of PSW ferroelectric ceramics by varying combination of  $\text{Pb}^{2+}$ ,  $\text{Sr}^{2+}$  and  $\text{W}^{6+}$  to make it best candidate for Opto-electronic applications.

## ACKNOWLEDGEMENT

The authors are grateful to Prof.C.F.Desai and UGC for Research Fellowship for doing this research work.

## REFERENCES

1. Benguigui L and Bethel K 1969 *J. Appl. Phys.* **47** 2787.
2. Takahashi M 1971 *Japan. J. Appl. Phys.* **10** 643
3. AMuñoz, *J. Phys.: Condens. Matter* **14** (2002) 8817-8830
4. W. R. Buessem, L. E. Cross, A. K. Goswami, *J. Am. Ceram. Soc.*, **75**, 2927 (1966)
5. Ahmad Safari, Rajesh K. Panda, and Victor F. Janas. *Ferroelectric Ceramics : Processing, Properties & Applications*.
6. Santiago, M, et al, *Physics Status Solids (A)*; Vol. 167, p.233-236, 1998.
7. Zha Shaowa et al, *Ceram. Int.* **27**, 649, 2001.



# Hydrothermal preparation and Photoluminescence of bundle-like structure of CdWO<sub>4</sub> nanorods.

Dhaval Modi<sup>†</sup>, D.Tawde and M.Srinivas

Physics Department, Faculty of Science, The M.S.University of Baroda, Vadodara-390002, Gujarat, India.

<sup>†</sup>Corresponding author: [bgjdmodi@gmail.com](mailto:bgjdmodi@gmail.com)

## Abstract

*CdWO<sub>4</sub> nanorods with a bundle like structure were synthesized at 95 °C for 12 h by hydrothermal process from 0.1 M Na<sub>2</sub>WO<sub>4</sub>.2H<sub>2</sub>O and CdCl<sub>2</sub>.H<sub>2</sub>O. The synthesized bundle-like structure of CdWO<sub>4</sub> nanorods were characterized by X-ray diffraction (XRD), Transmission electron microscopy (TEM). The luminescence properties of the bundle-like structure of CdWO<sub>4</sub> nanorods were investigated by photoluminescence (PL) spectroscopy.*

**Keywords:** Hydrothermal process, CdWO<sub>4</sub>, Photoluminescence

## Introduction

Because of metal tungstates have good application prospects in scintillators, optical fibers, microwave applications, humidity sensors, photoluminescence materials, and catalysts, etc. [1-4] Cadmium tungstate (CdWO<sub>4</sub>) with a monoclinic wolframite structure is one of the families of metal tungstates. It is a popular functional material because of its low radiation damage, high average refractive index and high X-ray absorption coefficient [5]. At room temperature, CdWO<sub>4</sub> shows photoluminescence (PL) whose peak is about 460 nm and has been used as an X-ray scintillator.[6] As a scintillator, its advantages, such as high efficiency, short decay time, high chemical stability and high stopping power make CdWO<sub>4</sub> irreplaceable.[7] Recently, because of its potential use as an advanced medical X-ray detector in computerized tomography [8] it has attracted special interest. CdWO<sub>4</sub> is a

monoclinic crystal structure with intermediate divalent cations and has been described as an ABX<sub>4</sub> structure, whose crystals are of the wolframite structure and not the scheelite structure. The monoclinic cell contains two CdWO<sub>4</sub> units. The divalent Cd has the usual octahedron configuration whose distances are close to the standard one. W has a very distorted coordination polyhedron: four O atoms are at the same distance and two are at different distances. The two distant O atoms were usually excluded from the first coordination sphere of W and were assigned to that of Cd. [9]

## Experimental

The sample was synthesized by hydrothermal method. Appropriate amount of 0.1M CdCl<sub>2</sub>.H<sub>2</sub>O (Cadmium Chloride) with distilled water was put in a Teflon-lined stainless steel autoclave of 90 ml capacity. The solution was stirred for 1 h and 0.1 M Na<sub>2</sub>WO<sub>4</sub>.2H<sub>2</sub>O (Sodium Tungstate) solution was added drop wise with strong magnetic

stirring. The autoclave was filled with distilled water up to 70% of the total volume. The autoclave was sealed and maintained at 95°C for 12 h, then cooled to room temperature naturally. The obtained white precipitate was centrifuged and washed with distilled water and absolute ethanol to remove any impurities, then dried at room temperature.

**Characterization of CdWO<sub>4</sub>**

**X-ray diffraction**

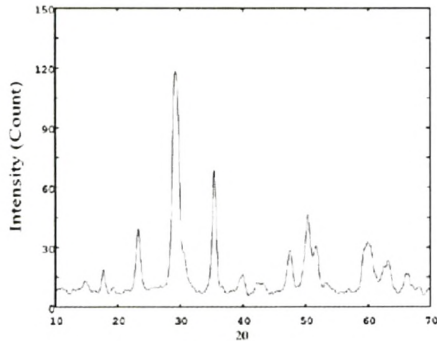


**Fig. 1** XRD patterns of CdWO<sub>4</sub> prepared at 95°C for 12 h

The XRD measurements were carried out with a Japan Rigaku D/max X-ray diffractometer, using Ni-filtered Cu K $\alpha$  radiation. A scan rate of 0.05°/s was applied to record the patterns in the 2 $\theta$  range 10-70°. XRD patterns revealed that the CdWO<sub>4</sub> can be indexed to the monoclinic wolframite structure with space group P2/c (13) and cell parameters are:

a : 5.01100

b : 5.80400

c : 5.05000

$\beta$  : 91.620; in agreement with the respective JCPDS (Joint Committee on Powder Diffraction Standards) card No. 01-080-0139. According to the literature [10, 11], XRD patterns are able to estimate the degree of structural order-disorder at long-range in the materials. Therefore, the strong but not sharp

peaks indicate that the CdWO<sub>4</sub> powder is crystallized in nature.

**Transmission electron microscopy**

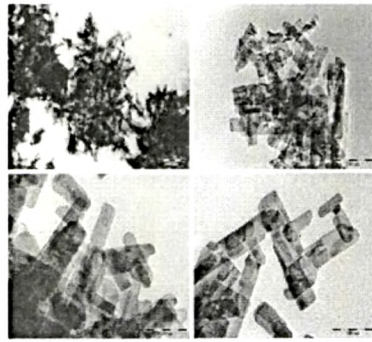


**Fig.2** TEM images of CdWO<sub>4</sub> prepared at 95°C for 12 h

The morphologies of the as-synthesized CdWO<sub>4</sub> are demonstrated in the TEM images shown in Fig.3. It is clear that these CdWO<sub>4</sub> nanorods self-assemble into bundle-like structures. The length of the CdWO<sub>4</sub> nanorod is approximately 80-220 nm and the width is about 50nm.

**Photoluminescence Studies**

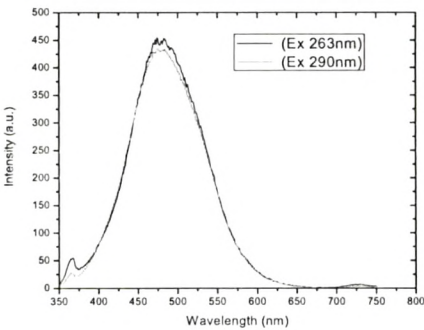


**Fig.3** PL spectra (with the excitation wavelength 263 nm and 290nm) of CdWO<sub>4</sub> prepared at 95°C for 12 h

Fig.3 shows photoluminescence spectroscopy emission spectrum for as-synthesized sample.

It exhibits a very strong emission peak at 480nm when excited the sample with 263 and 290nm. A shoulder peak is observed at 366nm. It is suggested that the blue emission originated from  $\text{WO}_4^{2-}$  complex. The intensities of PL emission depend strongly on preparation conditions. Further studies of the formation and growth mechanism of the nano rods are underway.

### Conclusions

$\text{CdWO}_4$  was synthesized by hydrothermal process at 95 °C for 12 h. XRD patterns revealed that the  $\text{CdWO}_4$  can be indexed to the monoclinic wolframite structure with space group P2/c (13). It is suggested that the blue emission originated from  $\text{WO}_4^{2-}$  complex. TEM images show that  $\text{CdWO}_4$  nanorods self-assemble into bundle-like structures.

### Acknowledgements

Dhaval Modi is thankful to Dr. K.V.R.Murthy (Applied Physics Department, M.S.University) for PL study and Dr.N.P.Lalla (UGC-DAE CSR Indore) for TEM characterization to carry out this research work.

### References

1. S.J. Chen, J.H. Zhou, X.T. Chen, J. Li, L.-H. Li, J.-M. Hong, Z.L. Xue, X.-Z. You, *Chem. Phys. Lett.* 375, 185 (2003)
2. S. Kwan, F. Kim, J. Akana, *Chem. Commun.* 447 (2001)
3. B. Liu, S.-H. Yu, F. Zhang, L.J. Li, Q. Zhang, L. Ren, K. Jiang, *J. Phys. Chem. B* 108, 2788 (2004)
4. X.L. Hu, Y. Zhu, *J. Langmuir* 20, 1521 (2004)
5. H. Lotem, Z. Burshtein, *Opt. Lett.* 12, 561 (1987)
6. Pustovarov, V. A.; Krymov, A. L.; Shulgin, B. *Rev. Sci. Instrum.* **1992**, 63, 3521.
7. Tanaka, K.; Miyajima, T.; Shirai, N.; Zhang, Q.; Nakata, R. *J. Appl. Phys.* **1995**, 77 (12), 6581.
8. Greskovich, C. D.; Cusano, D.; Hoffman, D.; Riedner, R. *J. Am. Ceram. Soc. Bull.* **1992**, 71, 1120.
9. Chicagov, A. P.; Ilyukhin, V. V.; Belov, N. *Sov. Phys. Dokl.* **1966**, 11, 11.
10. A.P.A. Marques, F.C. Picon, D.M.A. Melo, P.S. Pizani, E.R. Leite, J.A. Varela, E. Longo, *J. Fluoresc.* 18 (2008) 51.
11. I.L.V. Rosa, A.P.A. Marques, M.T.S. Tanaka, D.M.A. Melo, E.R. Leite, E. Longo, J.A. Varela, *J. Fluoresc.* 18 (2008) 239.

# STRUCTURAL AND PHOTOLUMINESCENCE PROPERTIES OF $\text{SrWO}_4$ MICROCRYSTALLITES PREPARED BY HYDROTHERMAL METHOD

Dhaval Modi<sup>†</sup>, D.Tawde and M.Srinivas

Physics Department, Faculty of Science, The M.S.University of Baroda, Vadodara-390002, Gujarat, India.

<sup>†</sup>*Corresponding author:* bgjdmodi@gmail.com

## ABSTRACT

$\text{SrWO}_4$  powder was synthesized by hydrothermal process at  $90^\circ\text{C}$  for 12 h Teflon lined Stainless steel autoclave. The obtained powder was characterized by X-ray diffraction (XRD), scanning electron microscopy (SEM) and photoluminescence (PL). XRD pattern of  $\text{SrWO}_4$  exhibits a scheelite-type tetragonal structure. SEM image shows flake like structure of  $\text{SrWO}_4$  microcrystallites. Photoluminescence emission spectra exhibits an intense peak around 365nm and a shoulder peak at 470nm.

**Keywords:** Hydrothermal process,  $\text{SrWO}_4$ , Photoluminescence

## INTRODUCTION

At room temperature, the tungstate presents a scheelite-type tetragonal structure with general formula  $\text{ABO}_4$  ( $A = \text{Ba, Ca, Sr, Pb}$ ;  $B = \text{W}$ ) and space group  $I41/a$  [1, 2]. In this type of structure, the B ions are within tetrahedral O-ion cages and isolated from each other, while the A ions are surrounded by eight oxygen [3]. Presently, these materials have been widely employed in various industrial applications, like: optical fiber, catalysts, scintillation detector, humidity sensor, solid-state lasers, photo catalysts, photoluminescent devices and more [4–6]. In particular,  $\text{SrWO}_4$  has attracted considerable attention to the development of new electro optics devices due to its blue or green luminescence emissions at room temperature [7].

## EXPERIMENTAL PROCEDURE

The sample was synthesized by hydrothermal method. Appropriate amount of  $0.1\text{M}$   $\text{SrCl}_2 \cdot 6\text{H}_2\text{O}$  (Strontium Chloride) with distilled water was put in a Teflon-lined stainless steel autoclave of 90 ml capacity. The solution was stirred for 1 h and  $0.1\text{ M}$   $\text{Na}_2\text{WO}_4 \cdot 2\text{H}_2\text{O}$  (Sodium Tungstate) solution was added drop wise with strong magnetic stirring. The autoclave was filled with distilled water up to 70% of the total volume. The autoclave was sealed and maintained at  $90^\circ\text{C}$  for 12 h, then cooled to room temperature naturally. The obtained white precipitate was centrifuged and washed with distilled water and absolute ethanol to remove any impurities, then dried at room temperature.

## CHARACTERIZATION

The morphologies were characterized using Scanning electron microscopy (SEM). Phase identification was conducted by the X-ray diffraction (XRD) technique, using  $\text{Cu K}_\alpha$  radiation by Rigaku X-ray diffractometer. SEM images were taken with Hitachi S-3000N Scanning electron microscope. The luminescence and excitation spectra of the sample were determined by a Fluorescence spectrometer with Xe lamp at R.T.

## RESULTS AND DISCUSSION

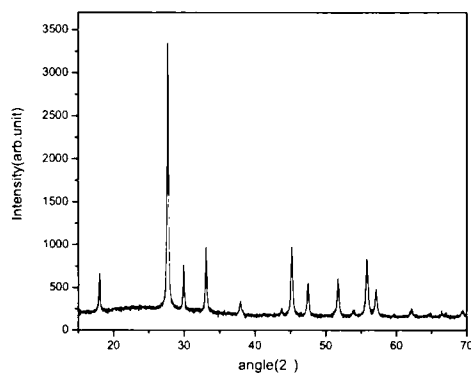


**Figure 1** XRD patterns of SrWO<sub>4</sub> powder.

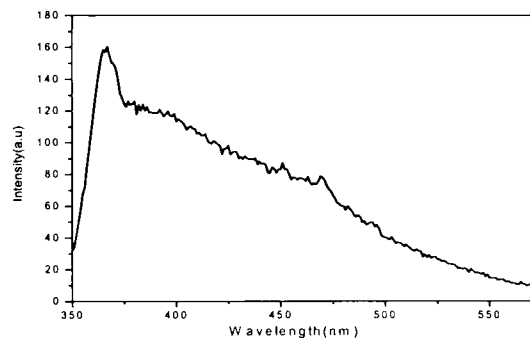
According to the literature [9, 10], XRD patterns are able to estimate the degree of structural order–disorder at long-range in the materials. Therefore, the strong and sharp peaks indicate that the SrWO<sub>4</sub> is highly crystallized and structurally ordered at long-range.

### *Photoluminescence Studies (PL)*

Blasse and Grabmaier [11] reported that the PL emission arises from the radiative return to the ground state, phenomenon that is in concurrence with the non-radiative return to the ground state. In the non-radiative process, the energy of the excited state is used to excite the vibrations of the host lattice, i.e., heat the lattice. The radiative emission process occurs more easily if there are trapped

### *X-ray Diffraction (XRD)*

Powder X-ray diffraction (XRD) patterns were recorded with a Japanese Rigaku D/max-RB diffractometer using Cu K $\alpha$  radiation ( $\lambda=0.15406$  nm) in the  $2\theta$  range from  $15^{\circ}$  to  $70^{\circ}$ . Fig. 1 shows the XRD pattern of SrWO<sub>4</sub> processed at  $90^{\circ}\text{C}$  for 12 h. XRD patterns revealed that the SrWO<sub>4</sub> powders can be indexed to the scheelite-type tetragonal structure with space group  $I4_1/a$ , in agreement with the respective JCPDS (Joint Committee on Powder Diffraction Standards) card No. 08-0490 [8].

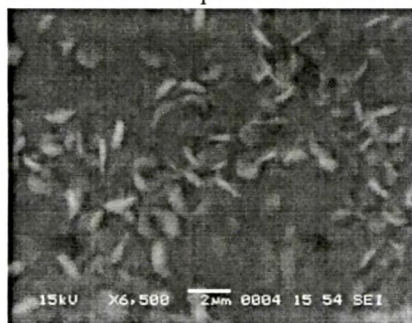


holes or trapped electrons within the band gap [12]. **Figure 2** Photoluminescence spectra

Fig.2 shows the photoluminescence (PL) spectrum at room temperature of SrWO<sub>4</sub> processed at  $90^{\circ}\text{C}$  for 12 h. Excitation of SrWO<sub>4</sub> was done with 248 nm wavelength. Photoluminescence emission spectrum exhibits an intense peak around 365nm and a shoulder peak at 470 nm. PL emission of tungstates with scheelite-type tetragonal structure is not completely understood.

In particular, the literature has reported several hypotheses to explain the mechanisms responsible by the PL emission of SrWO<sub>4</sub>. The existence of WO<sub>3</sub> and distorted WO<sub>4</sub> clusters in the SrWO<sub>4</sub> lattice, which are able to introduce the formation of intermediary energy levels are

composed of oxygen 2p states and tungsten 5d states. In this case, the polarization induced by the symmetry breaks and the existence of these localized energy levels are favorable conditions for the formation of trapped holes and trapped electrons. PL emission of  $\text{SrWO}_4$  with the transition of electrons within  $[\text{WO}_4]$  tetrahedron groups can be treated as excitons. The presence of some shoulders on the PL spectrum are interpreted as extrinsic transitions caused by the defects and/or impurities in the material.



*Scanning Electron Microscopy (SEM)*

Fig.3 shows the SEM micrograph of  $\text{SrWO}_4$  processed at  $90^\circ\text{C}$  for 12 hr. SEM micrograph revealed that the  $\text{SrWO}_4$  exhibits a large quantity of particles with agglomerate and flake like structure of  $\text{SrWO}_4$  microcrystallites.

**Figure 3** SEM micrograph of  $\text{SrWO}_4$

## CONCLUSIONS

$\text{SrWO}_4$  was synthesized by hydrothermal process at  $90^\circ\text{C}$  for 12 h. XRD patterns revealed that the  $\text{SrWO}_4$  can be indexed to the scheelite-type tetragonal structure with space group  $I41/a$ . The intense PL emission of  $\text{SrWO}_4$  is responsible for the transition of electrons within  $[\text{WO}_4]$  tetrahedron groups. SEM image shows flake like structure of  $\text{SrWO}_4$  micro crystallites.

## ACKNOWLEDGMENT

Dhaval Modi is thankful to Dr. K.V.R. Murthy of M. S. University of Baroda for providing facility of Photoluminescence measurements to carry out research work presented here.

## REFERENCES

1. L. Sun, Q. Guo, X. Wu, S. Luo, W. Pan, K. Huang, J. Lu, L. Ren, M. Cao, C. Hu, J. Phys. Chem. C 111,532(2007).
2. M. Anicete-Santos, F.C. Picon, M.T. Escote, E.R. Leite, P.S. Pizani, J.A. Varela, E. Longo, Appl. Phys. Lett. 88 ,2119131(2006).
3. G. Zhang, R. Jia, Q. Wu, Mater. Sci. Eng. B 128,254(2006).
4. J. Yu, L. Qi, B. Cheng, X. Zhao, J. Hazardous Mater. 158 ,301(2008).
5. H. Fu, J. Lin, L. Zhang, Y. Zhu, Appl. Catal. A 306,58(2006).
6. R.C. Pullar, S. Farrah, N.M. Alford, J. Eur. Ceram. Soc. 27,1059(2007).
7. L. Chen, Y. Gao, Mater. Res. Bull. 42 ,1823(2007).
8. <http://www.icdd.com/profile/overview.htm>.
9. A.P.A. Marques, F.C. Picon, D.M.A. Melo, P.S. Pizani, E.R. Leite, J.A. Varela, E. Longo, J. Fluoresc. 18,51(2008).
10. I.L.V. Rosa, A.P.A. Marques, M.T.S. Tanaka, D.M.A. Melo, E.R. Leite, E. Longo, J.A. Varela, J. Fluoresc. 18,239(2008).
11. G. Blasse, B.C. Grabmaier, Luminescent Materials, Springer, Berlin, 1994.
12. E. Orhan, M. Anicete-Santos, M.A.M.A. Maurera, F.M. Pontes, C.O. Paiva-Santos, A.G. Souza, J.A. Varela, P.S. Pizani, E. Longo, Chem. Phys. 312,1(2005).



## Structural, Dielectric and Optical characterization of Perovskite $\text{Pb}_{0.3}(\text{Zn}_{0.35}\text{W}_{0.35})\text{O}_3$

Dhaval Modi, D.Tawde and M.Srinivas

Department of Physics, Faculty of Science, The Maharaja Sayajirao University of Baroda, Vadodara, 390002,

Gujarat, India.

Email: bgjdmodi@gmail.com

### Abstract

Polycrystalline  $\text{Pb}_{0.3}(\text{Zn}_{0.35}\text{W}_{0.35})\text{O}_3$  was prepared by high temperature solid state reaction technique. The variation of dielectric constant ( $\epsilon$ ) and loss tangent ( $\tan \delta$ ) were scanned with respect to frequency in the range 100Hz to 10MHz with varying temperature from 25 to 160°C. The sample under investigation gives characteristic peaks of photoluminescence around 510 and 765 nm wavelengths.

### INTRODUCTION

Lead based perovskite ferroelectric materials (ceramics) have been studied for more than thirty years, owing to their technological applications such as multilayer capacitors (MLCs), electro mechanical coupling devices and actuators due to their low temperature sinterability, high permittivity and low temperature coefficient of capacitance [1] and excellent optical properties [2]. Several efforts have been made to synthesize  $\text{Pb}(\text{B}'\text{B}'')\text{O}_3$  perovskite type materials[3-12]. In the present paper the effort has been made to produce perovskite phase of similar compound by substituting  $\text{Zn}^{2+}$  cation at B-sub lattice side with composition of  $\text{Pb}_{0.3}(\text{Zn}_{0.35}\text{W}_{0.35})\text{O}_3$  using high temperature solid state reaction technique. Dielectric properties of  $\text{Pb}(\text{Zn,W})\text{O}_3$  and effect of Mg/Fe substitution has already been studied by Woo-Joon Lee [13]. According to our knowledge, this is the first attempt made to study the optical properties of lead zinc tungstate  $\text{Pb}(\text{Zn,W})\text{O}_3$ . It should be noted that expression PZW in this paper indicates composition of perovskite instead of its structure.

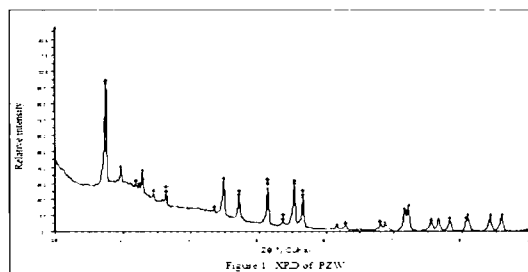
### EXPERIMENTAL

The sample was prepared by using  $\text{PbO}$ ,  $\text{ZnCO}_3$  and  $\text{WO}_3$  as starting reactants(>99.5% pure) with high temperature solid state reaction technique. The calcinations were performed in a closed ceramic crucible at 800°C for 12 h with heating rate of 200°C/hr. After calcinations samples were again grinded and then pellets of the size 13.72mm diameter and 1.45 mm thickness were prepared under the pressure of 5 ton without using any binding agent. Prepared pellet of PZW again sintered at 700°C temperature for 8 hrs. Dielectric properties of PZW was measured using 1260 Solartron Impedance analyzer. For better contact, surfaces of pellets as well as electrodes are silvered.

### RESULTS & DISCUSSION

#### Structural studies

Figure 1 Shows the X-ray diffraction pattern of PZW. The sample was characterized by Bruker AXS D8 advanced X-ray diffractometer using  $\text{Cu K}\alpha_1$  radiations. XRD peaks were indexed using standard JCPDS database. As prepared samples are of mixed phases of  $\text{PbWO}_4$  stolzite and respite,  $\text{Pb}_3\text{Zn}_2\text{WO}_9$ ,  $\text{ZnWO}_4$  type as indicated in the curve of X-ray pattern.



Failure of formation of PZW with perovskite is believed due to highly covalent nature of Zn, electro negativity difference and ionic size difference between Zn and Mg ions [4]

#### Dielectric properties

The detailed study of dielectric properties of PZW was measured using 1260 Solartron Impedance Analyzer. Frequency dependence of both real ( $\epsilon'$ ) and imaginary ( $\epsilon''$ ) parts of dielectric constant of PZW were studied and plotted against  $\log f$  for various temperatures starting from 25 to 160°C are shown in fig.2 and fig.3 respectively.

As shown in fig. 2 behaviour of real part of dielectric constant ( $\epsilon'$ ) was plotted against  $\log f$  for different temperatures. It is clear from the graph that  $\epsilon'$  has high value

for low frequency and it decreases with increase in frequency up to 100 kHz then becomes almost constant for remaining frequency region, which is the general behavior of ceramics[11,12].

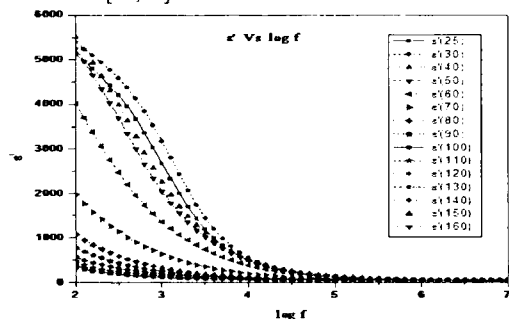


Figure 2 Behavior of real part of dielectric constant ( $\epsilon'$ ) with varying frequency and temperature

It is also observed from the figure that  $\epsilon'$  decreases sharply in low temperature region but it decreases slowly in high temperature region with increasing frequency up to 100 kHz, then becomes frequency independent.

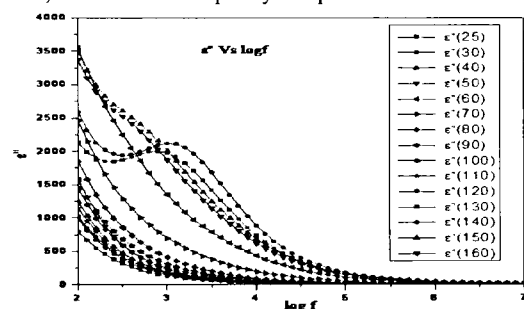


Figure 3 Behavior of imaginary part of dielectric constant ( $\epsilon''$ ) with varying frequency and temperature

Fig.3 shows behavior of imaginary part of dielectric constant ( $\epsilon''$ ) with frequency from 100Hz to 10 MHz.

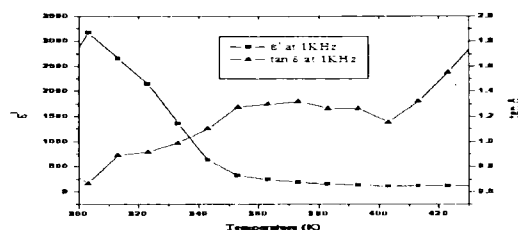


Figure 4 Behavior of  $\epsilon'$  and  $\tan \delta$  with temperature (K) at 1 kHz

Fig. 4 shows behavior of real part of dielectric constant and loss tangent ( $\tan \delta$ ) with different temperatures at constant frequency of 1 kHz.

### Optical properties

According to survey of literature, ours is the first attempt to study optical properties of PZW sample. Room temperature photoluminescence (PL) spectrum of the PZW is taken from JASCO 6300 spectrofluorometer at excitation wavelength of 305nm. A strong green emission and weak red emission

were observed. The green emission is assumed to be

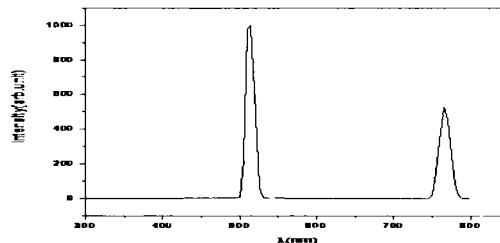


Figure 5 Photoluminescence of PZW at room temperature

connected with the inclusions of respite phase [6-9]. Red shift is observed in our sample which is very similar to the heavily  $\text{La}^{3+}$ -doped  $\text{PbWO}_4$  crystals [10]. It can be assumed that  $\text{Zn}^{2+}$  enters  $\text{PbWO}_4$  lattice creates Pb deficiency and contracted the optical band gap of PZW due to introduction of an extra recombination centers and traps in localized region.

### CONCLUSIONS

Perovskite phase of  $\text{Pb}_{0.3}(\text{Zn}_{0.35}\text{W}_{0.35})\text{O}_3$  can not be formed in this composition with high temperature solid state reaction technique. The sample under study exhibits high dielectric constant at low temperature which makes PZW a potential applicant as a dielectric material in capacitors and in memory cells to hold digital information. Red shift in PL spectra suggests its use for infrared detectors.

### REFERENCES

- Chen SY, Wang CM, Cheng SY, Mater Chem Phys.49 (1997) 70.
- Kuwata J, Uchino K, Nomura S, Ferroelectrics. 22 (1979) 863-867.
- Fyodorov A, Korshik MV, Missevitch O, et al, Radiat Meas. 26 (1996) 107.
- Smith WF, Principle of Material Science and Engineering, 2nd edn. (McGraw-Hill, Singapore, 1990) p37.
- Groenink JA, Blasse G, J Solid State Chem.39(1980) 9.
- Itoh M, Fujita M Phys Rev B. 62(2000)12825-12830.
- Itoh M, Alov DL, Fujita M, J Lumin. 87-89(2000) 1243-1245.
- Alov DL, Klassen NV, Kolesnikov NN, et al Proc Int Conf Inorg Scinti App. The Netherlands; (1996) p.267.
- Alov DL, Rybchenko SI, Mater Sci Forum. 279 (1997) 239-241.
- Li W, Feng X, Huang Y, J Phys: Condens Matter. 16 (2004) 1325-1333.
- Patankar KK, Mathe VL, Mahajan, RP et al, Mater Chem Phys.72(2001)23.
- Patankar KK, Dombale PD, Mathe VL et al, Mater Sci Eng. B87 (2001) 53-58.
- Lee Woo-Joon, Kim Jee-Su, Kim Nam-Kyoung. J Eur Ceram Soc. 27(2007) 3713-3717.